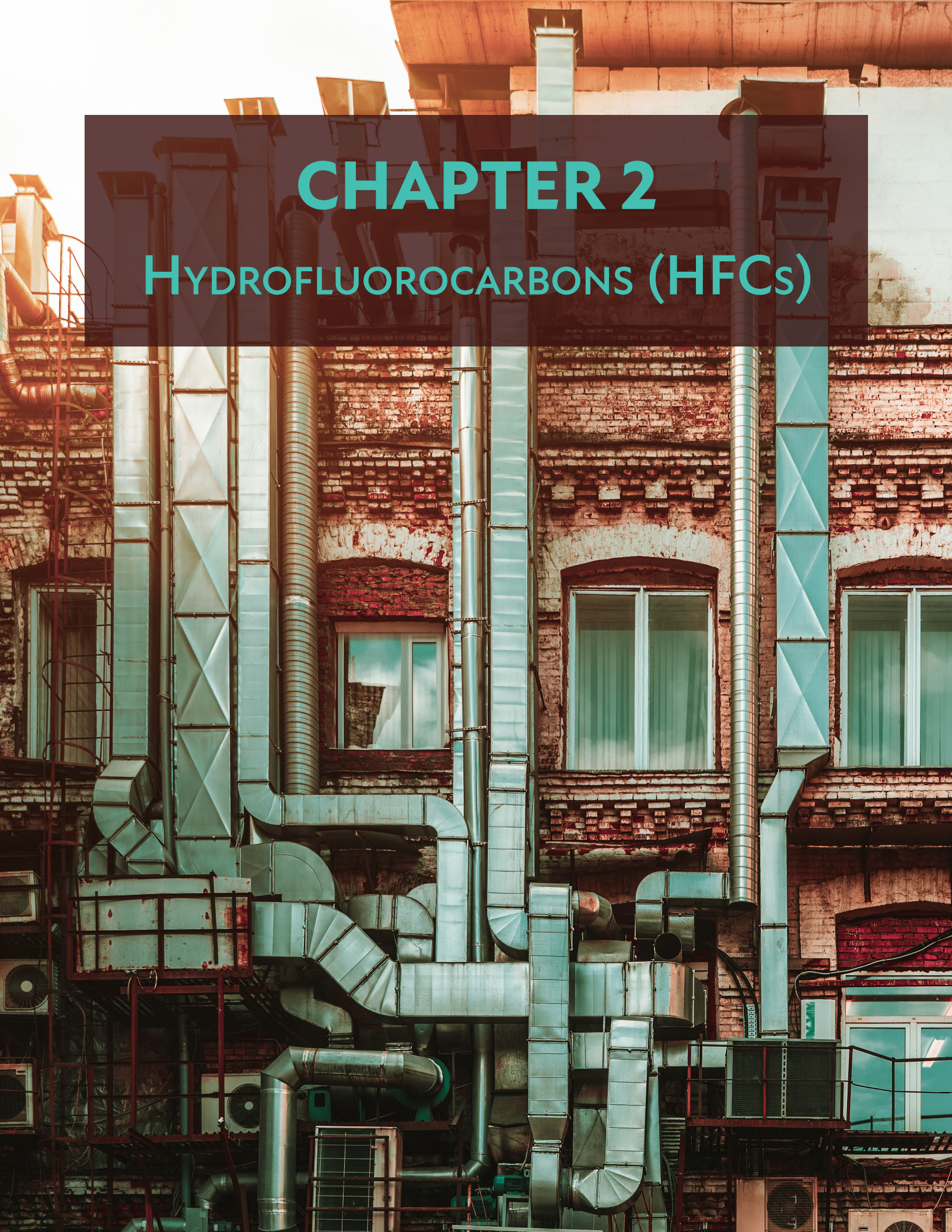

CHAPTER 2

Hydrofluorocarbons (HFCs)

About the cover image:
Hydrofluorocarbons (HFCs), widely used in the air conditioning and refrigeration sectors, are now controlled under the Kigali Amendment of the Montreal Protocol.

Photo credit: Adapted from image by skyNext via Adobe Stock

CHAPTER 2

Hydrofluorocarbons (HFCs)

Lead Authors : Qing Liang
Matthew Rigby

Coauthors : Xuekun Fang
David Godwin
Jens Mühle
Takuya Saito
Kieran M. Stanley
Guus J. M. Velders

Contributing Authors : Peter Bernath
Nada Derek
Stefan Reimann
Isobel J. Simpson
Luke Western

Review Editors : Stephen A. Montzka
Martin K. Vollmer

CONTENTS

Chapter 2: Hydrofluorocarbons (HFCs)

SCIENTIFIC SUMMARY

Hydrofluorocarbons (HFCs) have been increasingly produced and used in applications such as refrigeration, air-conditioning, and foam blowing following the phasedown of ozone-depleting substances (ODSs). In addition to emissions resulting from these uses, some HFCs, particularly HFC-23, are released as by-products during the manufacture of other compounds. While being benign for the stratospheric ozone layer and generally having lower radiative efficiencies than the most abundant ODSs, long-lived HFCs are potent greenhouse gases. Therefore, HFCs were included in the basket of substances controlled by the 1997 Kyoto Protocol under the United Nations Framework Convention on Climate Change (UNFCCC). Subsequently, certain HFCs were brought into the Montreal Protocol framework by the Kigali Amendment in 2016. The Kigali Amendment, which came into force in January 2019 for parties who ratified the Amendment, seeks to limit the production and consumption of a selection of HFCs. For HFC-23, the Kigali Amendment seeks to limit emissions formed as a by-product of HCFC (hydrochlorofluorocarbon) and HFC production to the extent practicable using approved technologies.

For the most abundant HFCs (HFC-134a, HFC-23, HFC-32, HFC-125, and HFC-143a) and some of the less abundant HFCs, atmospheric observations have been available for several years or decades. Observations in the remote atmosphere can be used to derive "top-down" global emissions. These emissions can be compared to the sum of "bottom-up" estimates derived from accounting methods for Annex I parties to the UNFCCC, who are required to report their emissions annually. For some parts of the world, atmospheric observations exist in sufficient density to derive top-down emissions estimates at regional scales. These can be compared to bottom-up estimates reported by the countries in these regions.

Based on the historical emissions trends derived from atmospheric data and estimates of future consumption, projections of future emissions can be derived under different policy scenarios. These emissions scenarios can be used to estimate the climate impact of various HFC policies in terms of future radiative forcing and temperature change.

The key findings of this chapter are as follows:

- **Global mean abundances of each of the major HFCs have increased since 2016.** Radiative forcing due to the HFCs reached 44.1 ± 0.6 mW m^{-2} in 2020, an increase of around one-third since 2016. HFC-134a remained the largest contributor to the overall radiative forcing due to HFCs (44%), and HFC-125 (18%) overtook HFC-23 (15%) as the second-largest contributor.
- **Total CO_2-equivalent HFC emissions inferred from observations increased through 2020.** The total carbon dioxide-equivalent emissions (CO_2-eq, calculated using 100-year global warming potentials, GWPs) due to HFCs was 1.22 ± 0.05 Pg CO_2-eq yr^{-1} in 2020 (1 Pg = 1 Gt), 19% higher than in 2016. Of this total, HFC-134a was responsible for approximately 30%, HFC-125 for 28%, HFC-23 for 20%, and HFC-143a for 15%. Emissions of the majority of HFCs grew between 2016 and 2020, except for HFC-143a, HFC-152a, HFC-365mfc, and HFC-43-10mee, for which emissions remained roughly constant. In 2020, global total CO_2-eq emissions due to HFCs were 60–70% higher than those of CFCs (chlorofluorocarbons) or HCFCs.
- **The gap between total CO_2-eq HFC emissions reported by Annex I countries to the UNFCCC and global estimates derived from atmospheric data has grown.** The emissions reported by Annex I countries in common reporting format (CRF) are approximately constant in the period 2015–2019, while atmospheric observations in the background atmosphere suggest continued growth in global total emissions. In 2019, UNFCCC reports accounted for only 31% (including HFC-23 in the analysis) or 37% (excluding HFC-23) of the global total CO_2-eq emissions derived from observations. Regional top-down emissions estimates for Europe, the USA, and Australia are similar to reported bottom-up emissions, suggesting that underreporting by these Annex I countries likely does not explain this discrepancy. Inverse modeling studies have been carried out for China and India (both non-Annex I countries) and find that around one-third of the emissions gap (excluding HFC-23) could be explained by sources in these countries. However, approximately 40% of global total HFC CO_2-eq emissions (excluding HFC-23) remain unaccounted for by Annex I reports or top-down estimates for non-Annex I parties. Top-down regional emissions estimates are available from only a relatively small number of countries based on the existing measurement network, whereas global top-down estimates reflect the aggregate of all emissions (for longer-lived HFCs). Therefore, the unattributed emissions probably occur in countries that are not monitored by atmospheric measurements and/or that do not report to the UNFCCC in CRF.
- **The global inferred CO_2-eq HFC emissions are less than the emissions in the 2018 Assessment HFC baseline scenario. They are about 20% lower for 2017–2019.** It is too early to link this directly to the provisions of the Kigali Amendment, since the first step in the scheduled phasedown was in 2019. The lower emissions can be explained by lower reported consumption in several countries following national regulations.
- **The ratio of global HFC-23 emissions inferred from atmospheric observations to reported HCFC-22 production has increased between 2010 and 2019, despite reports of substantial new emissions abatement since 2015.** Top-down estimates of global HFC-23 emissions were 17.2 ± 0.8 Gg yr^{-1} in 2019 (1 Gg = 1 kt). This is substantially larger than a bottom-up estimate of 2.2 Gg yr^{-1} derived from UNFCCC reports for Annex I countries (1.6 Gg yr^{-1}), HCFC-22 production reported to the United Nations Environment Programme (UNEP), and national abatement programs in India and China. The contribution to the global atmospheric

HFC-23 budget of photolysis of trifluoroacetaldehyde (CF_3CHO), a minor degradation product of some fluorinated compounds, is assessed to be negligible.

- **Some HFCs and unsaturated HFCs (hydrofluoroolefins [HFOs]) degrade in the environment to produce trifluoroacetic acid (TFA), a persistent toxic chemical.** HFO-1234yf has been increasingly used to replace HFC-134a as a mobile air conditioner (MAC) refrigerant. Measurements show that atmospheric background abundances of HFO-1234yf at Jungfraujoch, Switzerland have grown from less than 0.01 ppt before 2016 to annual median levels of 0.10 ppt in 2020. At the 2020 level, the oxidation of HFO-1234yf is likely producing a comparable, or potentially larger, amount of TFA than the oxidation of HFC-134a locally near Jungfraujoch. The measured and model simulated concentrations of TFA from the use of HFO-1234yf and other relevant HFOs, HFCs, HCFCs, and hydrochlorofluoroolefins (HCFOs) is, in general, significantly below known toxicity limits at present. However, the production of TFA in the atmosphere is expected to increase due to increased use of HFOs and HCFOs. Potential environmental impacts of TFA require future evaluation due to its persistence.
- **Projected emissions of HFCs based on current trends in consumption and emissions, national policies in several countries, and the Kigali Amendment are lower than those projected in the 2018 Assessment.** The 2020–2050 cumulative emissions in the 2022 updated Kigali Amendment scenario are 14–18 Pg CO_2-eq lower than the corresponding scenario in the previous Assessment. The 2050 radiative forcing in a scenario that assumes no controls on HFCs, is 220–250 mW m^{-2} (termed the Baseline scenario in the previous Assessment). Radiative forcing in 2050 is reduced to 90–100 mW m^{-2} in the 2022 Kigali Amendment scenario, 30 mW m^{-2} lower than projected in the 2018 Kigali Amendment scenario. The new scenario follows national controls on the consumption and production of HFCs in non-Article 5 countries, reflects lower reported consumption in China, is based on updated historical information on the use of HFCs in non-Article 5 countries, uses observed mixing ratios through 2020 as a constraint, and includes assumptions about reduced use of HFCs for commercial and industrial refrigeration. The new scenario also assumes that all countries adhere to the provisions of the Kigali Amendment.
- **Under the provisions of the Kigali Amendment, current trends in consumption and emissions, and national policies, the contribution of HFCs to global annual average surface warming is projected to be 0.04 °C in 2100.** This is substantially lower than under the scenario without HFC control measures, for which a contribution of 0.3–0.5 °C was projected.
- **Concerted efforts to improve energy efficiency of refrigeration and air-conditioning equipment could lead to reductions in greenhouse gas emissions of the same order as those from global implementation of the Kigali Amendment.** These estimated benefits of improving energy efficiency are highly dependent on greenhouse gas emissions from local electric grids and the pace of decarbonization in the energy sector.

2.1 INTRODUCTION

2.1.1 Summary of Findings from Previous Assessments

The previous Ozone Assessment reported the continuing rise of hydrofluorocarbon (HFC) emissions through 2016 and the accelerating growth of HFC atmospheric abundances. Radiative forcing due to HFCs was estimated to be 0.030 W m^{-2} in 2016, 1% of the total anthropogenic forcing for all long-lived greenhouse gases. Global CO_2-equivalent (CO_2-eq) HFC emissions were estimated to be 0.88 ± 0.07 Pg CO_2-eq yr^{-1} in 2016, 23% higher than in 2012. The magnitude of the rise in total HFC CO_2-eq emissions was found to be larger than the decline from chlorofluorocarbons (CFCs) and hydrochlorofluorocarbon (HCFCs). This was driven primarily by increases in HFC-134a, HFC-125, HFC-23, and HFC-143a, the four most abundant HFCs in the atmosphere. Emissions reported to the United Nations Framework Convention on Climate Change (UNFCCC) accounted for less than half of the global total derived from atmospheric measurements in 2016. The remaining emissions were thought to have originated primarily from non-Annex 1 countries. Global emissions of HFC-23 were found to have varied substantially, primarily due to changing levels of abatement in non-Annex 1 countries brought about by the UNFCCC Clean Development Mechanism (CDM). Emissions of HFC-23 inferred from atmospheric observations or from inventories generally agreed well. Future emissions scenarios suggested that the Kigali Amendment and national and regional regulations could more than halve radiative forcing due to all HFCs, excluding HFC-23, by 2050, compared to the baseline scenario.

2.1.2 Scope

Following the controls on CFC and HCFC production and use under the terms of the Montreal Protocol, the production and use of HFCs, which do not contribute to ozone depletion, increased substantially. HFCs are primarily used in refrigeration, air-conditioning, and foam blowing. Minor applications include use as firefighting agents and propellants (see **Table 2-1**). Post-production emissions of HFCs can occur months to decades following their manufacture, depending on the application. Once emitted, many HFCs persist in the atmosphere for several years or longer, where they absorb outgoing infrared radiation and therefore contribute to radiative forcing of climate.

Owing to their influence on climate, HFCs are subject to a range of regulations and international protocols. While HFCs were included in a basket of compounds controlled under the Kyoto Protocol to the UNFCCC, limits were not placed on their emissions explicitly as controls related to the aggregated total greenhouse gas emissions from individual parties. In some regions, national or regional regulations are in place to limit HFC use (e.g., European F-gas regulations; EU, 2014). In 2019, the Kigali Amendment to the Montreal Protocol came into force (**Box 2-1**). The Amendment sets out a phasedown schedule for production and consumption of a select group of HFCs, with differing time frames for non-Article 5 [non-A5] and Article 5 [A5] parties. For HFC-23, which is primarily a by-product of HCFC-22 production, the Kigali Amendment states that emissions should be controlled to the maximum extent practicable using proven technologies.

In this chapter, updates are provided for observations of the atmospheric abundance of HFCs. Global emissions are inferred based on these observations, estimates of their atmospheric lifetimes, and simulations of their dispersion throughout the atmosphere. These "top-down" emissions are compared to UNFCCC reports and other inventory-based ("bottom-up") methods. Furthermore, recent scientific literature is assessed regarding regional top-down and bottom-up emissions estimates and factors affecting the atmospheric lifetime and breakdown products of HFCs. Global emissions estimates are compared to earlier projections and emissions scenarios, and new scenarios are developed, constrained by updated atmospheric data. Information is also presented on new uses of HFCs, HFC alternatives, and energy efficiency improvements.

In 2017, Decision XXIX/12 was adopted, requesting that the Assessment Panels provide information on production and consumption of certain HFCs not listed as controlled substances under Annex F of the Montreal Protocol. The HFCs that are the subject of this decision have Global Warming Potentials (GWPs) at least as large as that of the controlled HFC with the lowest GWP (that of HFC-152). Of the 162 HFCs listed in the Annex, about 110 species meet this criterion. However, since there is no information available on the production, consumption, or atmospheric abundance of these compounds, they are not addressed in this Assessment.

2.2 ATMOSPHERIC OBSERVATIONS AND DERIVED EMISSIONS ESTIMATES

The abundance of HFCs in the atmosphere is regularly monitored by global networks such as the Advanced Global Atmospheric Gases Experiment (AGAGE; e.g., Prinn et al., 2018) and the National Oceanic and Atmospheric Administration (NOAA; e.g., Montzka et al., 2015). These networks maintain independent calibration scales, which typically agree within a few percent. Global measurements of HFC-134a are also provided by the University of California, Irvine (UCI; Simpson et al., 2014). The historical abundance of many HFCs, before routine ambient measurements began, has been reconstructed by AGAGE and the University of East Anglia from measurements of the Cape Grim Air Archive and archived Northern Hemispheric air samples (e.g., Prinn et al., 2018 and references therein; Oram et al., 2017; Laube et al., 2010; Leedham Elvidge et al., 2018). Complementing these surface-based observations, satellite data from the Atmospheric Chemistry Experiment Fourier Transform Spectrometer (ACE-FTS) onboard SCISAT provide estimates of upper-tropospheric abundance of HFC-23 and HFC-134a (Fernando et al., 2019; Bernath et al., 2021; Harrison et al., 2021).

In this section, updates of surface- and space-based measurements of atmospheric HFC abundances are provided through 2020. Based on the data from the AGAGE and NOAA surface networks, updates of top-down (atmospheric data-based) global annual mean emissions estimates are provided. The methodology for deriving global emissions, global lower-tropospheric mean abundances, CO_2-equivalent (CO_2-eq) emissions, and radiative forcing (defined as stratosphere-adjusted radiative forcing as outlined in **Box 5-1**) are described in detail in *Section 1.0*. Unless otherwise specified, all ranges given here correspond to 1-sigma uncertainties.

Global emissions estimates are presented here through 2020, the year in which socioeconomic activity was reduced

Box 2-1. The Kigali Amendment (2016) to the Montreal Protocol

The phasedown of chlorofluorocarbons (CFCs) and hydrochlorofluorocarbons (HCFCs) under the Montreal Protocol has led to substantial benefits to climate (e.g., Velders et al., 2007). Growth in the use of hydrofluorocarbons (HFCs) as replacements for CFCs and HCFCs could offset some of these climate benefits (Velders et al., 2012). To preserve the benefits by minimizing future growth in radiative forcing due to HFCs, parties to the Montreal Protocol agreed to an Amendment in Kigali, Rwanda, in October 2016. The Kigali Amendment added 18 HFCs to the Montreal Protocol as controlled substances and set out a schedule to phase down their production and consumption, or, in the case of HFC-23, reduce by-product emissions. The Amendment, which entered into force on 1 January 2019, outlines an 80–85% reduction in global production and consumption by 2047, with respect to baselines as defined in the caption to **Box 2-1 Figure 1**. By September 2022, 138 parties had ratified, approved, or accepted the Kigali Amendment.

HFCs controlled by the Kigali Amendment include HFC-23, HFC-134, HFC-134a, HFC-143, HFC-245fa, HFC365mfc, HFC-227ea, HFC-236cb, HFC-236ea, HFC-236fa, HFC-245ca, HFC-43-10mee, HFC-32, HFC-125, HFC-143a, HFC-41, HFC-152, and HFC-152a. The Amendment specifies that emissions of HFC-23 generated during production of HCFCs or HFCs be destroyed to the extent practicable beginning January 2020.

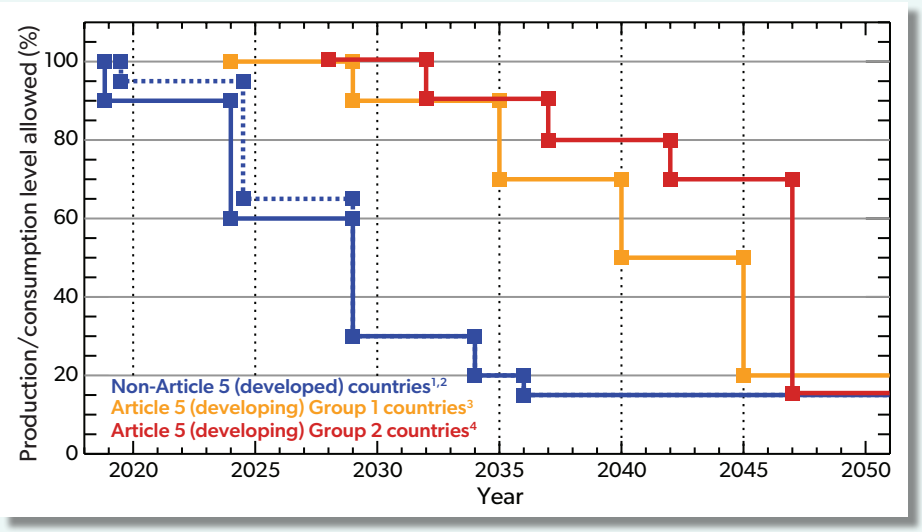

Box 2-1 Figure 1. Phasedown schedule for allowed production and consumption, in percentages with respect to defined baselines, of controlled HFCs, expressed as CO_2-equivalents (CO_2-eq), under the Kigali Amendment. The schedule for non-Article 5 (non-A5) countries is shown in blue[1,2], and the schedule for Article 5 (A5) countries is shown in orange[3] or red[4].

[1] Non-A5 countries also referred to as Article 2 countries (Article 2J of the Montreal Protocol). Baseline for non-A5 countries is defined as average HFC CO_2-eq production/consumption for 2011–2013 plus 15% of HCFC baseline in CO_2-eq production/consumption.
[2] For the non-A5 countries Belarus, Russian Federation, Kazakhstan, Tajikistan, and Uzbekistan, the baseline is defined as average HFC CO_2-eq production/consumption for 2011–2013 plus 25% of HCFC baseline CO_2-eq production/consumption (blue dotted line).
[3] Group 1: A5 countries not part of Group 2 (Article 5 of the Montreal Protocol). Baseline for A5 Group 1 countries is defined as average HFC CO_2-eq production/consumption for 2020–2022 plus 65% of HCFC baseline CO_2-eq production/consumption.
[4] Group 2: A5 countries are Bahrain, the Islamic Republic of Iran, Iraq, Kuwait, Oman, Pakistan, Qatar, Saudi Arabia, and the United Arab Emirates. Baseline for A5 Group 2 countries is defined as average HFC CO_2-eq production/consumption for 2024–2026 plus 65% of HCFC baseline CO_2-eq production/consumption.

in large parts of the world due to the COVID-19 pandemic. At present, there are very few peer-reviewed studies examining the influence of these restrictions on HFC emissions. Therefore, in this section, we do not speculate on the potential effect of the pandemic on HFC emissions.

Top-down regional emissions estimates are possible in parts of the world with sufficiently dense atmospheric measurement networks. In contrast to global inverse modeling, top-down regional emissions estimates of long-lived HFCs are insensitive to uncertainties in atmospheric lifetimes because transport timescales between emissions and measurement are small compared to their rate of removal in the atmosphere (**Box 1-2**). Uncertainties in derived regional emissions are typically dominated by uncertainties in the 3-D chemical transport models used to simulate atmospheric dispersion and uncertainties in the meteorological fields used to drive the models.

In the following section, recent literature on top-down and bottom-up regional emissions are assessed and compared to emissions reported by Annex I Parties to the UNFCCC, where available. The Annex I UNFCCC reports contain annual bottom-up estimates of emissions from those countries. In most of these reports, emissions estimates are available for several individual HFC species. However, reported emissions for some species from some parties are grouped together as an "unspecified mix" of compounds. For many individual species and for aggregated totals, statistically significant differences are found

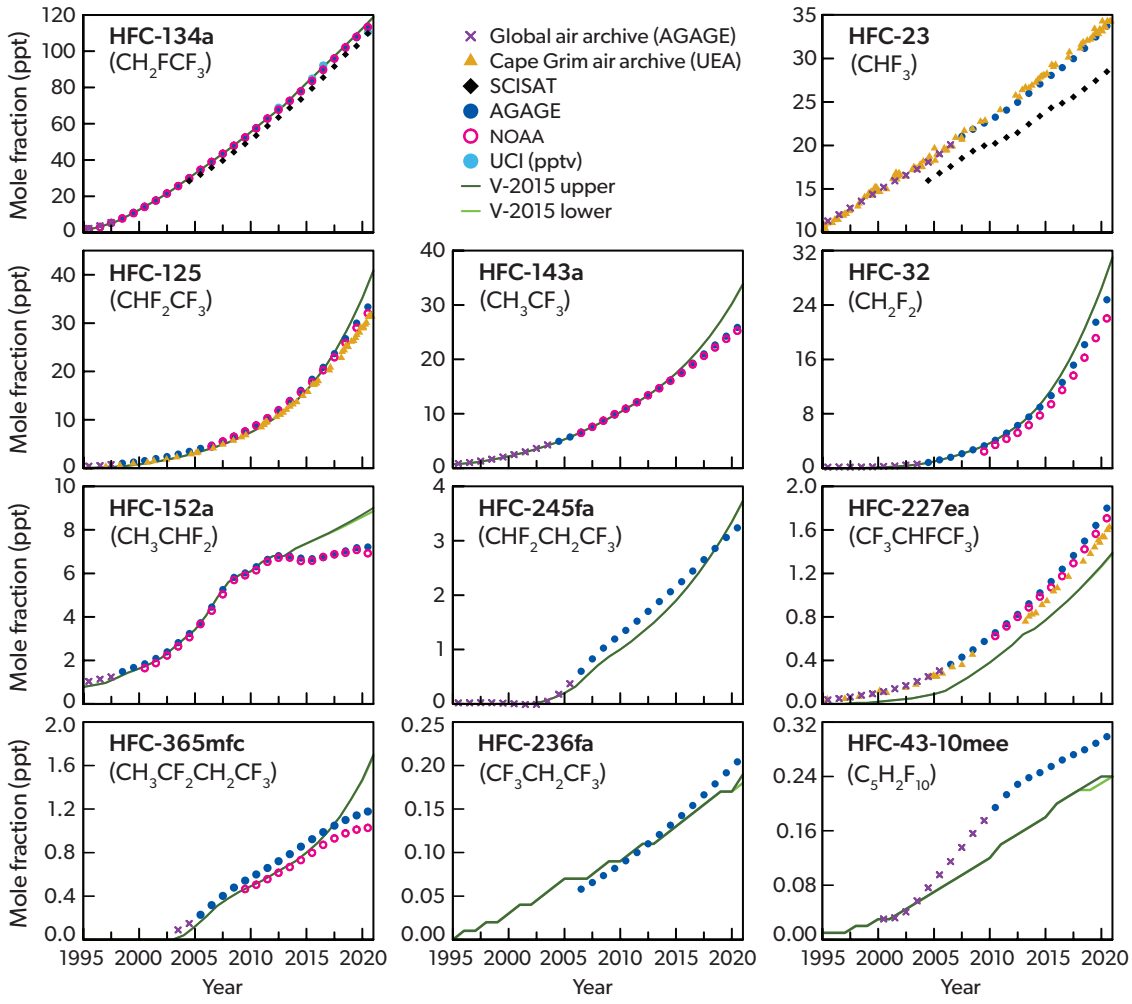

Figure 2-1. Annual mean mole fractions and recent projections. Global annual mean values from the independent ground-based AGAGE, NOAA, and UCI networks are shown as blue filled circles, magenta open circles, and light blue filled circles, respectively. AGAGE and NOAA values are based on monthly mean baseline measurements assimilated into the AGAGE global 12-box model (e.g., Rigby et al., 2014). Purple crosses represent global annual mole fractions based on AGAGE measurements of the Cape Grim Air Archive (CGAA) incorporated into the 12-box model. Gold triangles show Southern Hemisphere mole fractions from the CGAA measured by the University of East Anglia (UEA). Descriptions of these data can be found in Prinn et al. (2018) for AGAGE; Montzka et al. (2015) for NOAA; Simpson et al. (2014) for UCI; and Oram et al. (1998), Laube et al. (2010), and Leedham Elvidge et al. (2018) for UEA. UCI HFC-134a data are reported as pptv (parts per trillion, volume based). In contrast, AGAGE and NOAA data are reported as ppt (dry air mole fraction). Differences are expected to be small at the reported abundances compared to the stated 10% uncertainty of the UCI HFC-134a scale. Upper-tropospheric measurements from ACE-FTS aboard SCISAT represent averages for 60°S–60°N in the altitude range of 5.5–8.5 km for HFC-23 and 45°S–45°N in the altitude range of 10.5–14.5 km for HFC-134a (black diamonds, Fernando et al., 2019; Boone et al., 2020; Bernath et al., 2021). Since the previous Assessment, the ACE-FTS processing algorithm has been updated (Boone et al., 2020), which changed some trend values compared to previous versions (Bernath et al., 2021). ACE-FTS data are reported as wet air mole fractions. A water vapor correction was not applied to the ACE data as its influence is thought to be small compared to the other uncertainties. Also shown are projections from Velders et al. (2015; dark and light green lines).

between summed Annex I emissions reports and global top-down emissions, even when available regional top-down estimates of non-Annex I emissions are added to the Annex I reports. These gaps may arise from substantial emissions in non-reporting countries and, potentially from underreporting of emissions in reporting countries (although, as discussed below, where top-down estimates are available, substantial underreporting has not yet been identified).

Updates relating to the atmospheric lifetime and degradation products of HFCs are discussed in *Section 2.3*.

Table 2-1. Lifetimes, the 100-year time horizon GWP, and main applications of the HFCs with the highest atmospheric abundances.

Name	Formula	Lifetime (yr)	GWP-100	Main Applications
HFC-134a	CH_2FCF_3	14	1470	• Refrigerant for mobile and for domestic refrigerators/freezers • Blend component for stationary air-conditioning and commercial refrigeration • Propellant for pharmaceutical aerosols and for industrial aerosols • Blowing agent
HFC-23	CHF_3	228	14,700	• By-product in production of HCFC-22 • Low-temperature specialist refrigerant • Firefighting agent
HFC-32	CH_2F_2	5.4	749	• Blend component for air-conditioning equipment and commercial refrigeration and heat pumps
HFC-125	CHF_2CF_3	30	3820	• Blend component for stationary air-conditioning and commercial refrigeration and heat pumps • Firefighting agent
HFC-143a	CH_3CF_3	51	5900	• Blend component for commercial refrigeration
HFC-152a	CH_3CHF_2	1.6	153	• Propellant for specialized industrial aerosols • Blowing agent component for extruded polystyrene foams
HFC-245fa	$CHF_2CH_2CF_3$	7.9	966	• Foam blowing agent for polyurethane foams • Working fluid for organic Rankine cycles
HFC-365mfc	$CH_3CF_2CH_2CF_3$	8.9	969	• Foam blowing agent for polyurethane and phenolic foams • Blend component for solvents
HFC-227ea	CF_3CHFCF_3	36	3580	• Propellant for pharmaceutical aerosols • Firefighting agent
HFC-236fa	$CF_3CH_2CF_3$	213	9120	• Firefighting agent
HFC-43-10mee	$CF_3CHFCHFCF_2CF_3$	17	1610	• Solvent for specialized applications

Table 2-2. Global atmospheric mole fractions and emissions of hydrofluorocarbons estimated by surface air sampling networks.

Species	Network	Annual Mean Mole Fraction (ppt)			Change (2019–2020)		Emissions (2020)	
		2016	2019	2020	ppt yr^{-1}	% yr^{-1}	Gg yr^{-1}	Tg CO_2-eq yr^{-1}
HFC-134a	AGAGE	89.4	108	113	5.5	5.1	247 ± 28	364 ± 41
	NOAA	89.8	108	113	5.4	5.0	243 ± 27	358 ± 39
	UCI (pptv)	92.1	108	111	3.3	3.1		
HFC-23	AGAGE	28.9	32.5	33.7	1.3	3.9	17 ± 0.8	243 ± 12
HFC-125	AGAGE	20.9	30	33.3	3.3	11	92 ± 6	352 ± 23
	NOAA	20.2	29	32	3.0	10	83 ± 5	319 ± 20
HFC-143a	AGAGE	19.3	24.3	25.9	1.6	6.7	31 ± 2	185 ± 12
	NOAA	19	23.8	25.2	1.5	6.2	29 ± 2	169 ± 10
HFC-32	AGAGE	12.6	21.5	24.8	3.3	15	70 ± 7	53 ± 5
	NOAA	11.5	19.1	22	2.9	15	62 ± 6	47 ± 5
HFC-152a	AGAGE	6.73	7.18	7.21	0.032	0.44	54 ± 8	8.3 ± 1.2
	NOAA	6.75	7.08	6.92	–0.15	–2.1	49 ± 8	7.5 ± 1.1
HFC-245fa	AGAGE	2.44	3.06	3.24	0.18	5.9	14 ± 2	13 ± 2
HFC-227ea	AGAGE	1.24	1.64	1.8	0.16	9.7	6.3 ± 0.7	23 ± 3
	NOAA	1.17	1.56	1.71	0.14	9.1	5.8 ± 0.6	21 ± 2
HFC-365mfc	AGAGE	0.989	1.14	1.18	0.035	3.1	4.3 ± 1	4.1 ± 0.9
	NOAA	0.87	1.01	1.03	0.015	1.5	3.4 ± 0.7	3.3 ± 0.7
HFC-236fa	AGAGE	0.154	0.192	0.204	0.013	6.6	0.39 ± 0.09	3.5 ± 0.8
HFC-43-10mee	AGAGE	0.264	0.289	0.299	0.0099	3.4	1.2 ± 0.3	1.9 ± 0.5

Notes: Averages represent annual calendar-year global means for each independent measurement network. The AGAGE and NOAA networks share only a few common measurement sites; most measurements occur at different sites. Differences in the 2016 values since WMO (2018) are due to calibration scale changes and differences in methodology used to estimate global means. The observations are updated from Prinn et al. (2018) and Montzka et al. (2015). They are available at http://agage.mit.edu/ for AGAGE data and gml.noaa.gov/dv/site/ for NOAA data. Global means are estimated by assimilating data into the AGAGE 12-box model (Cunnold et al., 1983; Rigby et al., 2013), using the methodology of Rigby et al. (2014). UCI HFC-134a data are reported as pptv (parts per trillion, volume based; Simpson et al., 2014). In contrast, other data are reported as ppt (molar based). Differences are expected to be small at the reported abundances compared to the stated 10% uncertainty of the UCI HFC-134a scale.

2.2.1 Global and Regional HFC Abundances and Emissions

In this section, we provide updates to the abundance and emissions of each HFC species. Species are grouped in subsections based broadly on their application or production route and are ordered, approximately, by their contribution to radiative forcing.

2.2.1.1 HFC-134a (CH_2FCF_3)

HFC-134a is the most abundant HFC and contributes the most to total HFC radiative forcing. Its lifetime in the atmosphere is approximately 14 years, and its 100-year Global Warming Potential (GWP) is approximately 1470 (*Annex*). It is used as a refrigerant in mobile and domestic refrigerators and freezers, a blend component for stationary air-conditioning and commercial refrigeration, a foam-blowing agent, and a propellant for pharmaceutical and industrial aerosols (**Table 2-1**). In some applications, lower-GWP refrigerants, such as HFO-1234yf and HFO-1234ze(E), are starting to replace HFC-134a (UNEP, 2017).

The global annual mean mole fraction reached 113 ± 2 ppt in 2020, up from 89 ± 1 ppt in 2016 (average of AGAGE and NOAA data; UCI results over this period are 111 ± 2 ppt in 2020, up from 92 ± 2 ppt in 2016; **Table 2-2** and **Figure 2-1**). The change in mole fraction between 2016 and 2020 was 24 ± 2 ppt (26 ± 2%), which is similar, within uncertainty, to that during the four-year period (2012–2016) examined in the previous Assessment. This observed increase in global mole fraction is similar to that projected in Velders et al. (2015). The global abundance in 2020 contributed to a radiative forcing of 19.5 ± 0.3 mW m^{-2}, the highest of any HFC.

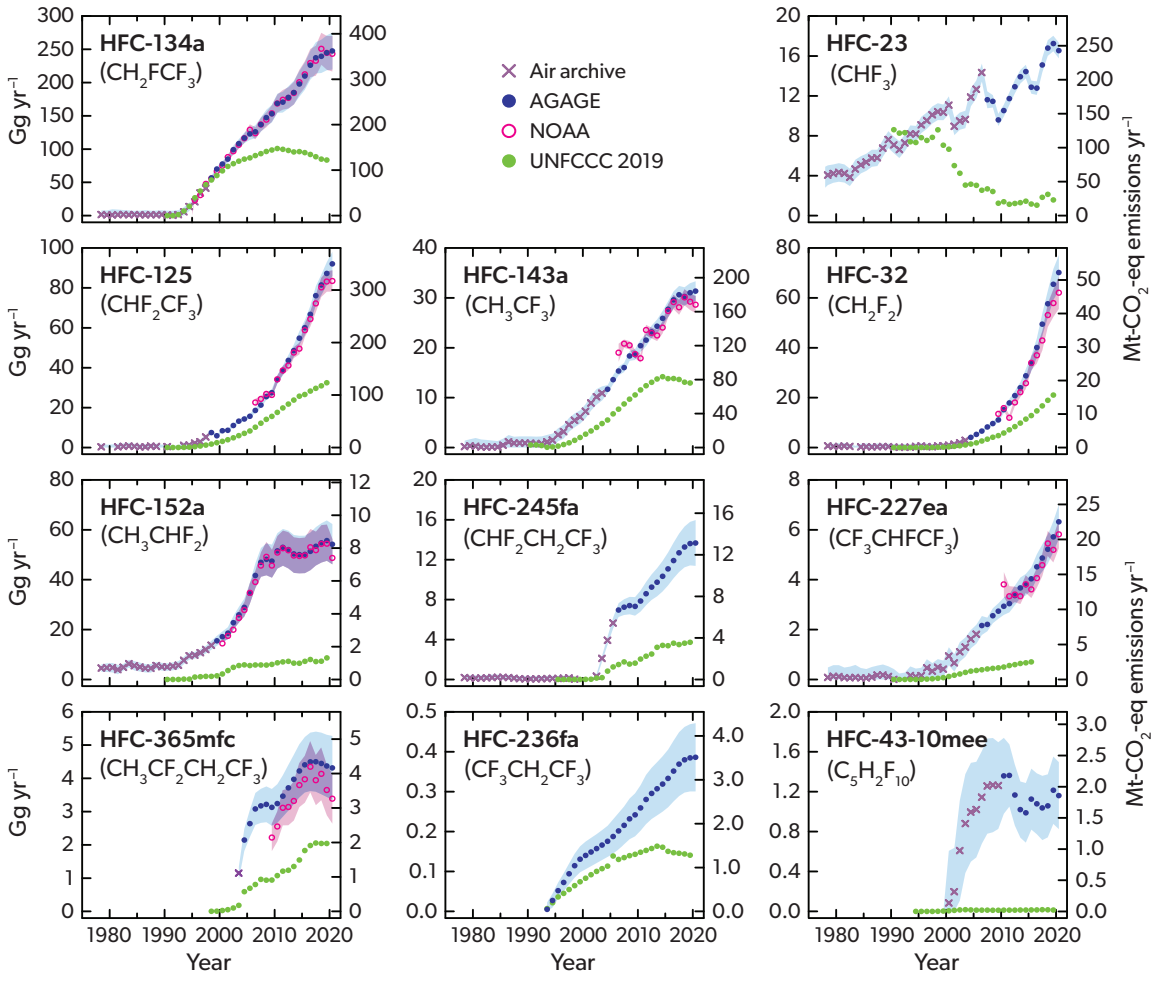

Figure 2-2. Global emissions derived from background atmospheric measurements and Annex I emissions reports to the UNFCCC. Emissions shown as blue circles are derived from five background AGAGE stations, filtered to remove measurements that are strongly influenced by regional sources. Purple crosses show global emissions derived from AGAGE measurements of the Cape Grim Air Archive. Red open circles show emissions derived from NOAA measurements in the remote atmosphere. Global emissions are derived from the AGAGE 12-box model, with steady state lifetimes as in **Table 2-1** and the *Annex*, using the method described in Rigby et al. (2014). Left-hand axes show emissions in Gg yr^{-1}, and the right-hand axes show CO_2-eq emissions. Shading indicates 1-sigma uncertainties and includes contributions from measurement and model error, as well as due to lifetime and calibration scale uncertainty. Green filled circles show the total emissions from Annex I countries reported to the UNFCCC (2019).

Upper-tropospheric distributions of HFC-134a between 45°S and 45°N in the altitude range 10.5–14.5 km are measured from orbit as mole fractions by ACE-FTS (Fernando et al., 2019; Bernath et al., 2021). The latitude and altitude ranges are different from those used in the previous Assessment (60°S to 60°N) due to ACE-FTS retrieval problems below 10 km. These observations indicate that HFC-134a in the upper troposphere increased from 85.5 ± 0.3 ppt in 2016 to 109.8 ± 0.2 ppt in 2020 (**Figure 2-1**; Fernando et al., 2019; Bernath et al., 2020; Harrison et al., 2021). Uncertainties in these quantities represent the standard deviation in the mean and do not include potential systematic errors, which are likely to be substantially larger. The upper-tropospheric trend observed from ACE-FTS is consistent with the trends derived from the surface-based AGAGE and NOAA measurements.

Total global emissions of HFC-134a estimated from inverse analysis of mole fractions at remote sites increased from 228 ± 21 Gg yr^{-1} in 2016 to 245 ± 27 Gg yr^{-1} in 2020 (average of AGAGE and NOAA inversions, which differ from each other by about 1%; **Table 2-2** and **Figure 2-2**). Previous Assessments noted a near-linear rise in HFC-134a emissions since the early 1990s. The updated observations indicate that the growth in emissions has slowed substantially since the previous Assessment (Montzka, Velders et al., 2018); the increase in emissions between 2016 and 2020 was approximately 18 ± 3 Gg yr^{-1} (8 ± 1%), compared to a rise of 51 ± 3 Gg yr^{-1} (28 ± 2%) between 2012 and 2016. The 2020 HFC-134a emissions were equivalent to 361 ± 40 Tg CO_2-eq yr^{-1}.

While global top-down emissions of HFC-134a have grown, the totals reported to the UNFCCC by Annex I countries have declined from 92 Gg yr^{-1} in 2016 to 84 Gg yr^{-1} in 2019 (the last year available at the time of writing). Therefore, the discrepancy between the UNFCCC reported emissions and global top-down values, noted in the previous Assessment, has increased to around 160 Gg yr^{-1} in 2019. This gap is approximately three times the total reported emissions (**Figure 2-3**). Montzka, Velders et al. (2018) described numerous regional top-down studies, which indicated that emissions from the major reporting regions, primarily the USA and Europe, were similar to, or slightly lower than, the emissions estimates reported to UNFCCC by these two regions. Therefore, it was proposed that the gap was most likely due to emissions from non-reporting countries, although it is possible that underreporting has occurred from Annex I countries that are not well observed by atmospheric measurement networks.

Atmospheric measurement–based emissions estimates for the USA and Europe were discussed in the previous Assessment. Since then, additional studies have become available that support the conclusion that underreporting by UNFCCC Annex I countries does not explain the discrepancy with global top-down estimates. In Europe, new measurements of HFC-134a were carried out on the island of Crete, and these were combined with long-term measurements in Ireland, Switzerland, and Italy (Schoenenberger et al., 2018). These measurements allowed new estimates to be made of emissions from central and western Europe and the eastern Mediterranean. The top-down estimates of aggregated HFC-134a emissions for reporting countries in the domain were 51% (37–69%) lower than the UNFCCC reports (total top-down emissions were 18.6 [16.7–20.6] Gg yr^{-1} for this domain). In Australia, top-down emissions of around 1 Gg yr^{-1} were derived, around half of the value reported to the UNFCCC (Dunse et al., 2018) and only ~0.4% of global total emissions.

For non-Annex I countries, new top-down and bottom-up estimates have become available for India and China only. Two

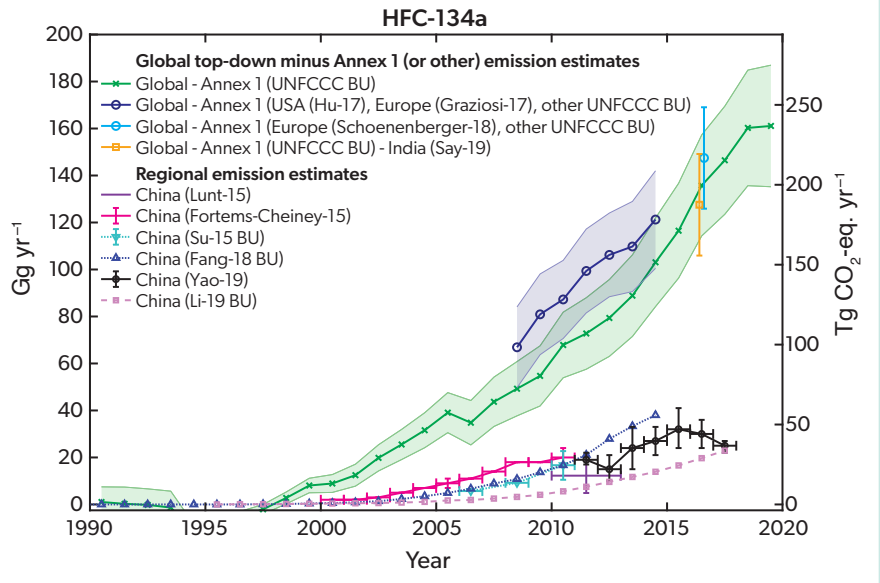

Figure 2-3. Difference between global HFC-134a emissions derived from atmospheric observations (AGAGE and NOAA mean) and UNFCCC reports from Annex I countries (green line and crosses with shading represent 1-sigma uncertainty). The dark blue line with open circles and shading shows the same but with UNFCCC reports for the USA and Europe replaced by regional inversion results from Hu et al. (2017) and Graziosi et al. (2017), respectively. Similarly, the light blue circle and error bar shows the global difference but with European UNFCCC reports replaced by top-down values from Schoenenberger et al. (2018). A set of bottom-up or top-down regional emissions estimates are shown for China in broken or solid lines, respectively. Top-down estimates are from Lunt et al. (2015) in purple, Fortems-Cheiney et al. (2015) in magenta, and Yao et al. (2019) in black. Bottom-up estimates are from Su et al. (2015) in dotted cyan, Fang et al. (2018) in dotted blue with triangular points, and Li et al. (2019) in a light pink dashed line with square data points. The contribution of emissions from India is indicated in the gold square and error bar, which represents the global top-down/UNFCCC difference minus the Indian emissions estimate from Say et al. (2019).

bottom-up studies by Li et al. (2019) and Fang et al. (2018) estimate rapidly increasing emissions of HFC-134a in China through 2017 and 2014, respectively (**Figure 2-4**). However, the estimates by Li et al. (2019) are about half that by Fang et al. (2018), at 14 Gg yr^{-1} and 38 Gg yr^{-1} in 2014, respectively. Top-down estimates by Yao et al. (2019) use flask and in situ measurements from seven observatories in China between 2011 and 2017. The top-down estimates also exhibit an increase during this period, although with substantial interannual variability. The average top-down emissions estimate from this study falls between the two bottom-up estimates, with emissions of 25 (22–27) Gg yr^{-1} for 2017. In India, air samples were collected at low altitudes during an aircraft campaign in June and July 2016 (Say et al., 2019). National emissions of HFC-134a derived from these observations were 8.2 (6.1–10.7) Gg yr^{-1}. Based on these top-down studies, India and China could account for around 25% of the difference between global top-down HFC-134a emissions estimates and UNFCCC reports (**Figure 2-3**). The remaining missing emissions probably occur in countries for which sparse atmospheric monitoring precludes the estimation of regional emissions and/or that do not report to the UNFCCC.

2.2.1.2 HFC-23 (CHF_3)

The radiative forcing due to HFC-23 was the third largest of the HFCs in 2020 (down from the second largest in the previous Assessment). It has the longest lifetime (228 years) and highest 100-year GWP (14,700) of the HFCs described here (*Annex*). In contrast to the other, more abundant HFCs, the majority of HFC-23 in the atmosphere has not been released following its intentional use (**Table 2-1**). Instead, it is primarily a by-product that is vented during the production of other compounds. The major focus of previous work on HFC-23 has been its emissions during the production of HCFC-22 (e.g., Oram et al., 1998; Miller et al., 2010; Miller and Kuijpers, 2011; Simmonds et al., 2018; Stanley et al., 2020). There is also evidence that HFC-23 can be released during the production of tetrafluoroethylene (TFE) and hexafluoropropylene (HFP) from HCFC-22 (Sung et al., 2006; Ebnesajjad, 2015; *Section 7.2.2.1*). However, there has not been an assessment of the quantities recycled within production facilities or potential contributions of these sources to global total emissions. Compared to by-product emissions from HCFC-22 production, smaller emissions are associated with the use of HFC-23 as a feedstock for halon-1301 production, as a plasma etching chemical and chamber-cleaning agent in the semiconductor industry, as a

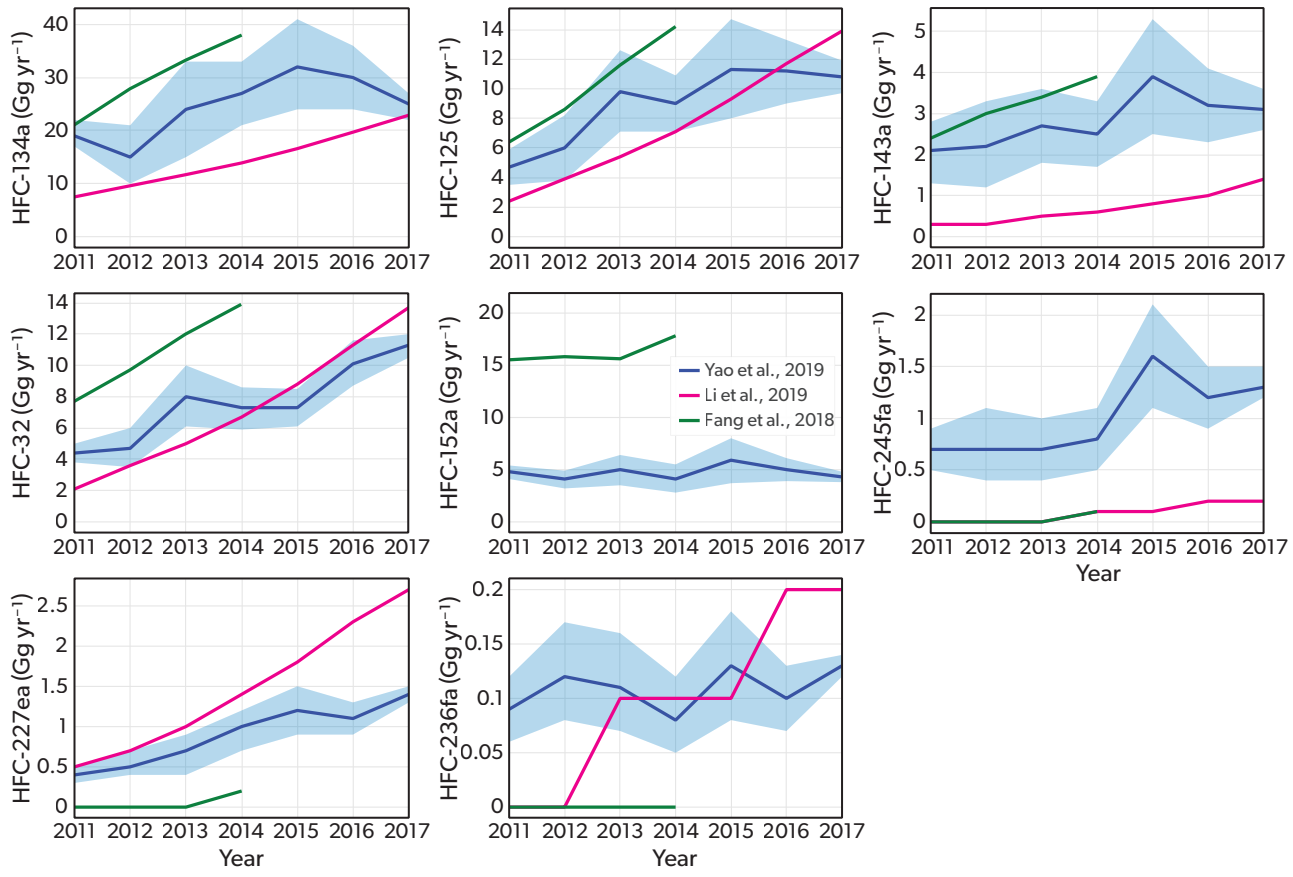

Figure 2-4. Emissions of the major HFCs (excluding HFC-23 and HFC-43-10mee) from China. Top-down estimates from Yao et al. (2019) are shown in blue, including 1-sigma uncertainties as shaded areas. Bottom-up estimates are from Li et al. (2019) in red and Fang et al. (2018) in green.

very low-temperature refrigerant, and as a specialty fire-suppression agent.

The abundance of HFC-23 continues to increase in the global atmosphere and reached 33.7 ± 0.9 ppt in 2020, compared to 28.9 ± 0.7 ppt in 2016 (AGAGE data; **Table 2-2** and **Figure 2-1**). The previous Assessment (Montzka, Velders et al., 2018) noted a reduction in growth rate from around 1.1 ppt yr^{-1} to 0.9 ppt yr^{-1} between 2014 and 2016. This trend has since reversed, with growth reaching 1.3 ppt yr^{-1} around 2018/19, the highest rate yet recorded (Stanley et al., 2020). The overall change in mole fraction between 2016 and 2020 was 4.8 ± 1.1 ppt (17 ± 4%), compared to 4.0 ± 1.0 ppt (16 ± 4%) between 2012 and 2016. The radiative forcing due to HFC-23 was 6.5 ± 0.2 mW m^{-2} in 2020.

HFC-23 concentrations in the upper troposphere from ACE-FTS through 2020 are shown in **Figure 2-1** (Fernando et al., 2019; Bernath et al., 2021). These upper-tropospheric means for latitudes 60°S and 60°N were approximately 15–20% lower than surface-based estimates from the AGAGE network. The ACE-FTS growth rate was also smaller than that observed in the AGAGE network, with an increase from 2016 to 2020 of 3.6 ± 0.1 ppt (14 ± 1%). As with HFC-134a, the uncertainties quoted here represent the standard deviation in the mean and do not include potential systematic errors, which are likely to be substantially larger. Ground-based column-average observations of HFC-23 based on FTIR measurements at Rikubetsu, Japan, and Syowa Station, Antarctica (Takeda et al., 2021), exhibited similar trends to those based on the AGAGE measurements at similar latitudes, but the column mole fractions were around 15% lower on average.

The previous Assessment (Montzka, Velders et al., 2018) noted a decline in emissions derived from remote AGAGE measurements between 2014 and 2016. Stanley et al. (2020) found that this trend had since reversed and that emissions had grown to 15.9 ± 0.9 Gg yr^{-1} in 2018. Updates presented here show an additional rise to 17.2 ± 0.8 Gg yr^{-1} in 2019, and a similar value of 16.5 ± 0.8 Gg yr^{-1} in 2020 (**Table 2-2** and **Figures 2-2** and **2-5**). The 2020 emissions of HFC-23 were equivalent to 243 ± 12 Tg CO_2-eq yr^{-1}.

Global inventory-based (bottom-up) emissions estimates are derived from publicly accessible information, as outlined in Stanley et al. (2020) and shown in **Figure 2-5**. For Annex I parties to the UNFCCC, annual HFC-23 emissions reports are available (UNFCCC, 2021). For countries not obliged to report to the UNFCCC, HFC-23 by-product generation is calculated by multiplying reported HCFC-22 production by estimates of HFC-23 by-product formation per mass of HCFC-22 produced. From these totals, reported abatement is subtracted, based on information from the UNFCCC Clean Development Mechanism (CDM) or national programs.

For Annex I parties to the UNFCCC, reported emissions have been relatively low during the last decade. Other than in 2018, reported emissions have remained below 2 Gg yr^{-1} since 2008. Between 2016 and 2018 growth was reported, predominantly driven by emissions from fluorochemical production. However, a decrease to 1.6 Gg yr^{-1} was subsequently reported in 2019 (**Figure 2-2**).

HCFC-22 production totals and HFC-23 by-product weights were taken from information provided to UNEP under Article 7 of the Montreal Protocol and made publicly available through reports of the UN Multilateral Fund (MLF; UNEP, 2018a, 2018b) and the Technology and Economic Assessment panel (TEAP; UNEP, 2020b). The TEAP report suggests that China is the largest producer of HCFC-22, accounting for 61% of global production in 2018; India is the next largest, accounting for less than 10% (UNEP, 2020b). The HCFC-22 production amounts from China suggest the generation of 14 Gg yr^{-1} of HFC-23 by-product in 2018 (UNEP, 2020a).

Between 2006 and 2014, the amount of HFC-23 by-product abated before reaching the atmosphere was taken from CDM reports (Stanley et al., 2020). Since 2015, China has reported to the MLF increasing HFC-23 abatement at its HCFC-22 production facilities, reaching 45%, 93%, 98%, and 99.8% HFC-23 destruction in 2015, 2016, 2017 and 2018, respectively (UNEP, 2018a, 2018b, 2020c). An executive order in India required HCFC-22 producers to destroy all HFC-23 by-product from October 2016 onward (MEFCC, 2016).

These bottom-up considerations suggest an overall growth of HFC-23 by-product generation from non-Annex I countries between 1990 and 2019 (**Figure 2-5**, dashed red line), reflecting an increase in global total HCFC-22 production. However, when abatement is considered, a substantial reduction in emissions to the atmosphere is estimated during the CDM period (2006–2014) and from 2015 (**Figure 2-5**, top panel, solid red line). Updated global bottom-up emissions were 2.2 Gg yr^{-1} in 2019. The previous Assessment (Montzka, Velders et al., 2018) presented substantially lower bottom-up HFC-23 emissions in 2014 and 2015 (based on Simmonds et al., 2018) than is shown here. This disagreement is due to revisions in reported HCFC-22 production and HFC-23 by-product weights that resulted from verification programs that occurred since the last Assessment (UNEP, 2018a, 2018b, 2020c). Furthermore, it was assumed in the estimates used in the previous Assessment that abatement installed during the CDM period would continue after the scheme closed, whereas the updated estimates rely only on reported abatement amounts.

Up until 2013, global bottom-up emissions track (within ± 2 Gg yr^{-1}) the global emissions derived from atmospheric measurements (**Figure 2-5**, top panel; Miller et al., 2010; Simmonds et al., 2018; Stanley et al., 2020). Similarly, up until 2013, the ratio of HFC-23 emissions to HCFC-22 production (E_{23}/P_{22}) derived from atmospheric data closely matched that derived from bottom-up estimates (**Figure 2-5**, bottom panel). As reported in Stanley et al. (2020), between 2013 and 2015, top-down emissions grew more slowly than expected based on HCFC-22 production data and the decline in abatement reported under the CDM, which had been operating since 2006. They proposed that this change can be explained by new emissions from newly installed, and at least partly unabated, HCFC-22 production capacity, combined with the switching off of some, but not all, abatement installed before or during the CDM period. Between 2015 and 2019, as reported abatement increased dramatically in China and India, bottom-up emissions and E_{23}/P_{22} declined substantially (**Figure 2-5**). However, emissions and E_{23}/P_{22} derived from atmospheric data increased. By 2019, the difference between top-down and bottom-up emissions and E_{23}/P_{22} was the largest since atmospheric records began. Stanley et al. (2020) concluded that this discrepancy was most likely the result of the reported emissions abatement, primarily from China, not being fully realized, or substantial new unreported HCFC-22 production. Stanley et al.

(2020) estimated that only 27% of the reported global abatement capacity was achieved in 2018.

A small number of regional top-down studies have provided additional information on the spatial distribution of global HFC-23 emissions. However, none of these studies can explain the discrepancy between bottom-up and top-down global emissions after 2016. Using aircraft data collected over India in June and July 2016 (prior to the Indian government's executive order to incinerate HFC-23 by-product from HCFC-22 production), Say et al. (2019) derived emissions of 1.2 Gg yr^{-1} for a region in the northern part of the country comprising 72% of the Indian population and four of five known HCFC-22 manufacturing plants. In China, Pu et al. (2020) carried out observations in the Yangtze River Delta region between 2012 and 2016. They estimated that their measurements were sensitive to the Shanghai, Zhejiang, Jiangsu, and Anhui provinces, as well as to nine fluorine chemistry plants producing HCFC-22, comprising around 46% of national emissions. Using a tracer ratio method, with carbon monoxide as the reference tracer, emissions of 2.4 ± 1.4 Gg yr^{-1} were derived for this region. Manning et al. (2021) derived United Kingdom (UK) emissions of HFC-23 that were not statistically different from zero for most years between 2008 and 2020. The derived emissions were broadly consistent with the UK National Inventory Report, which suggests very small emissions (<0.1 Gg yr^{-1}).

2.2.1.3 HFC-32 (CH_3F_2), HFC-125 (CHF_2CF_3), HFC-143a (CH_3CF_3)

Current radiative forcing due to HFC-32, HFC-125, and HFC-143a, which are primarily used as HCFC substitutes in refrigerants (**Table 2-1**), are the fifth, second, and fourth largest of the HFCs, respectively. They have lifetimes of 5.4, 30, and 51 years and 100-year GWPs of 749, 3820, and 5900 (*Annex*). The abundances of all three compounds have increased in the background atmosphere since the previous Assessment, with global surface mean mole fractions in 2020 of 23.4 ± 0.7 ppt for HFC-32, 32.7 ± 1.6 ppt for HFC-125, and 25.6 ± 0.8 ppt for HFC-143a (AGAGE and NOAA mean; **Figure 2-1** and **Table 2-2**). The increases between 2016 and 2020 were 11.4 ± 0.8 ppt (94 ± 4%), 12.1 ± 1.9 ppt (59 ± 7%), and 6.4 ± 1.0 ppt (33 ± 4%), respectively. Except for HFC-143a, these increases are larger, in absolute terms, than the change between 2012 and 2016. However, they are smaller than the increases projected by Velders et al. (2015; second row of **Figure 2-1**), which was the basis for the baseline scenario for HFC projections in the previous Assessment. The radiative forcings in 2020 due to these species were 3.0 ± 0.1 mW m^{-2} (HFC-32), 8.0 ± 0.4 mW m^{-2} (HFC-125), and 4.4 ± 0.1 mW m^{-2} (HFC-143a).

Global top-down emissions in 2020 were 66 ± 7 Gg yr^{-1} for HFC-32, 88 ± 6 Gg yr^{-1} for HFC-125, and 30 ± 2 Gg yr^{-1} for HFC-143a (mean of AGAGE and NOAA inversions, **Figure 2-2**). The increases in their emissions between 2016 and 2020 were 28 ± 1 Gg yr^{-1} (72 ± 2%), 22 ± 1 Gg yr^{-1} (34 ± 1%), and 0.6 ± 0.9 Gg yr^{-1} (2 ± 3%), respectively. The year-to-year emissions growth rate declined during this four-year period for all three compounds. HFC-143a exhibited the most marked slowdown, with overall growth not significantly different from zero between 2016 and 2020. The 2020 emissions of these substances were equivalent to 50 ± 5 Tg CO_2-eq yr^{-1} (HFC-32), 335 ± 22 Tg CO_2-eq yr^{-1} (HFC-125), and 177 ± 11 Tg CO_2-eq yr^{-1} (HFC-143a).

Since the previous Assessment, emissions reported to the UNFCCC have increased for HFC-32 and HFC-125 (reaching 21

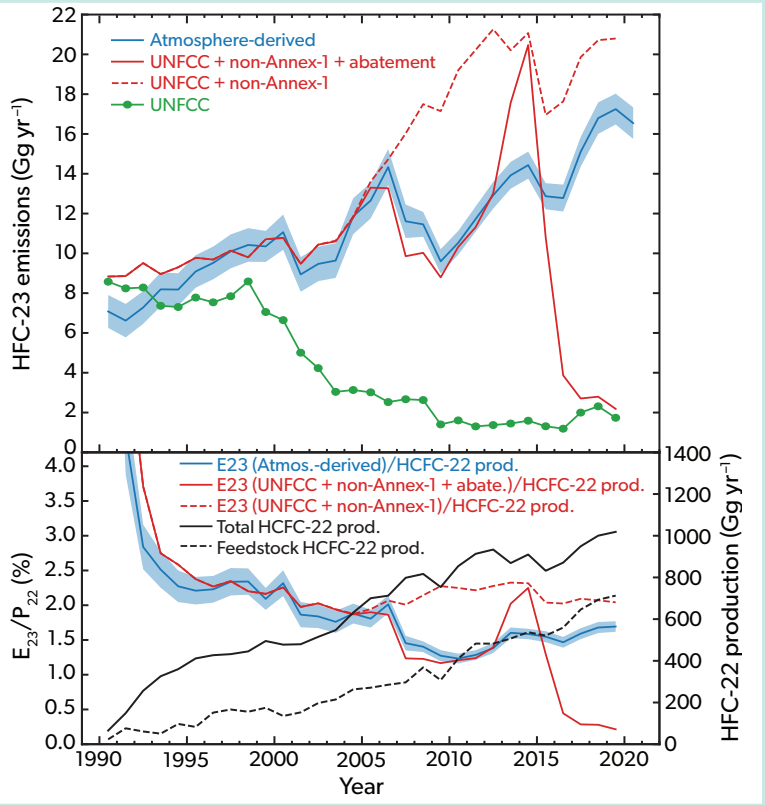

Figure 2-5. HFC-23 global emissions and HFC-23/HCFC-22 production ratio (updated from Stanley et al., 2020). *(top panel)* Top-down emissions estimates derived from AGAGE data are shown in blue (1-sigma uncertainty shown in blue shading). The dashed red line shows the sum of emissions reported to the UNFCCC and a bottom-up estimate for non-Annex I countries based on HCFC-22 production reported to the Multilateral Fund (MLF) and an HFC-23 emissions factor. The solid red line shows the same but includes abatement of HCFC-22 production-related emissions. Abatement estimates are derived from reports under the UNFCCC Clean Development Mechanism, reports to the MLF of abatement after 2015 by China and the assumed complete abatement of HCFC-22 production emissions in India due to an executive order in 2016. Emissions reported to the UNFCCC (2021) are shown in green. *(lower panel)* Total (solid black line) and feedstock (dashed black line) production of HCFC-22 (right-hand axis). The blue line shows the ratio of top-down HFC-23 emissions to HCFC-22 production (E23/P22). The solid and dashed red lines show the same, but for E23 derived from bottom-up methods either with (solid) or without (dashed) the reported abatement, respectively.

Gg yr^{-1} and 32 Gg yr^{-1} in 2019, respectively), and have slightly fallen for HFC-143a (13 Gg yr^{-1} in 2019). The drop in reported emissions for HFC-143a likely follows from a reduction in its use in the European Union (EU) ahead of its 2020 phaseout in favor of lower-GWP alternatives in commercial refrigeration (Velders, et al., 2022; *Section 2.4.1*). The gap between these reports and global emissions derived from atmospheric observations has grown for all three species (**Figures 2-6** to **2-8**). For 2019, UNFCCC reports represented 34%, 38%, and 43% of global top-down emissions for HFC-32, HFC-125, and HFC-143a, respectively.

Updated top-down emissions have been derived for several UNFCCC Annex I countries. These studies support the conclusions of the previous Assessment that the gap between reported and top-down emissions could not be explained by underreporting to the UNFCCC for countries that are monitored by atmospheric observations. Top-down estimated emissions of HFC-125 and HFC-143a in 2013 were smaller than, or consistent with, the reported emissions for central and western Europe and the eastern Mediterranean (Schoenenberger et al., 2018). For the UK, top-down emissions estimates were lower than inventory-based estimates for HFC-125 and HFC-32 from the early 2000s to 2018 (Manning et al., 2021). For HFC-143a, the top-down values were similar to the UNFCCC reported emissions between 2010 and 2016, but in the subsequent years, top-down values rose above inventory estimates. For all three gases, UK emissions were estimated to be less than 2% of the global total derived from AGAGE and NOAA observations. Similarly, top-down emissions for Australia were estimated to be less than 2% of global emissions for each of these gases between the early 2000s and 2016 (Dunse et al., 2018). Substantial over-reporting of HFC-125 was found in the Australian inventory (top-down values around 50% lower) and underreporting for HFC-32 and HFC-143a (top-down estimates two to three times higher).

Among non-Annex I countries that do not regularly report to the UNFCCC, top-down or bottom-up studies have been conducted in China, India, and South Africa. These studies suggest that some, but not all, of the gap between the global top-down estimates and UNFCCC reports can be explained by emissions from these countries (**Figures 2-6** to **2-8**). In China, growing top-down emissions of HFC-32, HFC-125, and HFC-143a were derived for 2011 to 2017, reaching 11.3 (10.5–12.0) Gg yr^{-1}, 10.8 (9.7–11.9) Gg yr^{-1}, and 3.1 (2.6–3.6) Gg yr^{-1}, respectively, at the end of the study period (Yao et al., 2019). These emissions could explain around 20–40% of the difference between UNFCCC reports and the global top-down estimates for these gases. Similar to HFC-134a, the top-down estimates for HFC-125 and HFC-143a emissions from China of Yao et al. (2019) mostly fall between inventory-based estimates of Li et al. (2019) and Fang et al. (2018), while the HFC-32 emissions estimates are slightly lower in recent years. Based on a spatially and temporally sparse aircraft dataset collected during the summer of 2016, Say et al. (2019) estimated Indian emissions of 6.4 (5.2–7.8) Gg yr^{-1} for HFC-125 and 0.8 (0.4–1.2) Gg yr^{-1} for HFC-143a. These emissions could account for around 5–17% of the global difference between top-down estimates and UNFCCC reports for these two species. For HFC-32, Say et al. (2019) derived Indian emissions that were only ~2% of the gap. Using measurements from Cape Point, Kuyper et al. (2019) estimated small emissions of HFC-125 from South Africa (~1% of global emissions, after extrapolation of emissions derived in the vicinity of Cape Point to the whole country based on population density).

2.2.1.4 HFC-152a (CH_3CHF_2)

HFC-152a is the seventh-largest contributor to radiative forcing of the HFCs. Compared to the other major HFCs, it has a relatively short atmospheric lifetime of 1.6 years and a low GWP (relative to other HFCs) of 153 over a 100-year time horizon (*Annex*). This species is mainly used as a propellant for specialized industrial aerosols, as a blowing agent component for extruded polystyrene foams, and recently as a replacement for HFC-134a in some automobile air-conditioning systems (**Table 2-1**).

As reported in the previous Assessment (Montzka, Velders et al., 2018), the growth of HFC-152a in the background atmosphere slowed substantially between 2012 and 2016 compared to the preceding decade. This trend has continued, with HFC-152a exhibiting a relatively small increase of 0.33 ± 0.29 ppt (5 ± 4%) between 2016 and 2020, reaching 7.1 ± 0.2 ppt in 2020 (mean of AGAGE and NOAA data; **Figure 2-1** and **Table 2-2**). This slowdown contrasts with the projected continuing growth during this period in Velders et al. (2015). The radiative forcing of climate due to HFC-152a was 0.9 ± 0.03 mW m^{-2} in 2020.

Global emissions of HFC-152a derived from observations in the background atmosphere did not change significantly between 2016 and 2020. They were 51 ± 8 Gg yr^{-1} in 2020, a change of –0.7 ± 0.9 Gg yr^{-1} (–1 ± 2%) relative to 2016 (AGAGE and NOAA mean; **Figure 2-2**). Although HFC-152a has the fourth-largest mass emissions of the HFCs because of its relatively short lifetime and lower (relative to other HFCs) GWP, the CO_2-equivalent emissions of HFC-152a were only the ninth largest in 2020, at 8 ± 1 Tg CO_2-eq yr^{-1}.

Emissions of HFC-152a reported to the UNFCCC have increased slightly since those reported in the previous Assessment (8.6 Gg yr^{-1} in 2019 compared to 7.3 Gg yr^{-1} in 2015; **Figure 2-2**), but the substantial discrepancy between top-down and reported emissions remains, at 46 Gg yr^{-1} in 2019. The UNFCCC reports accounted for 16% of the global top-down values in that year. As noted in the previous Assessment, much of this difference could be attributed to the USA not reporting HFC-152a emissions explicitly but instead aggregating them with several other compounds (including HFC-227ea, HFC-245fa, and HFC-43-10mee). Regional top-down studies confirmed that substantial emissions (~10–30 Gg yr^{-1}) originated from the USA around the period 2004–2012 (Stohl et al., 2009; Miller et al., 2012; Barletta et al., 2011; Lunt et al., 2015; Simmonds et al., 2016).

Recent top-down studies in Europe, the eastern Mediterranean, and Australia have confirmed that these regions are relatively small contributors to global total HFC-152a emissions. Emissions for western and central Europe and the eastern Mediterranean were inferred to be 2.8 (2.3–3.3) Gg yr^{-1} in 2013 (Schoenenberger et al., 2018), accounting for around 5% of global emissions. For Annex I countries in the domain, emissions were consistent with, or lower than, those reported to the UNFCCC. Emissions of less than 0.1 Gg yr^{-1} (or around 0.1% of global emissions) were inferred for Australia between 2003 and 2016 (Dunse et al., 2018).

Regional inverse estimates from the non-Annex I countries China and India suggest that emissions from these regions do not contribute substantially to the difference between the top-down global total and the global UNFCCC reports. Yao et al. (2019) made a top-down estimate of HFC-152a emissions in China, and these were generally consistent with top-down estimates

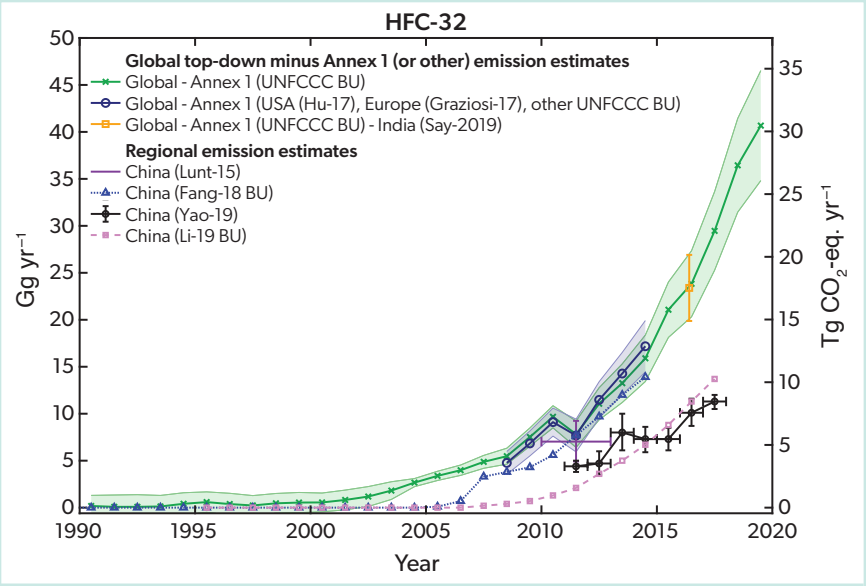

Figure 2-6. As in **Figure 2-3**, but for HFC-32.

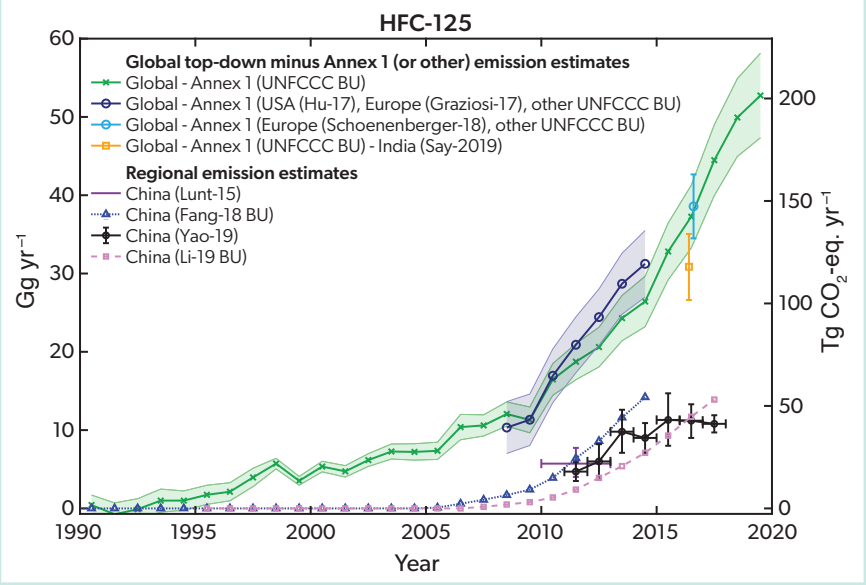

Figure 2-7. As in **Figure 2-3**, but for HFC-125.

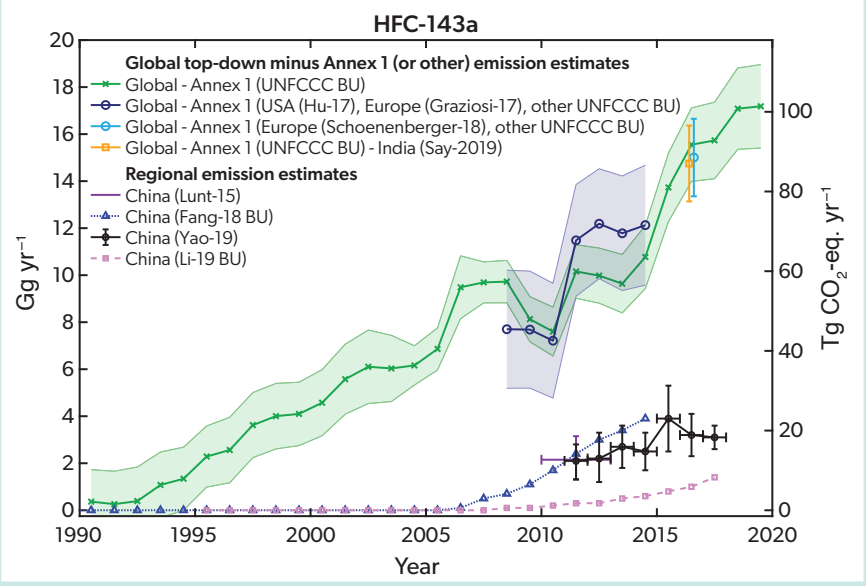

Figure 2-8. As in **Figure 2-3**, but for HFC-143a.

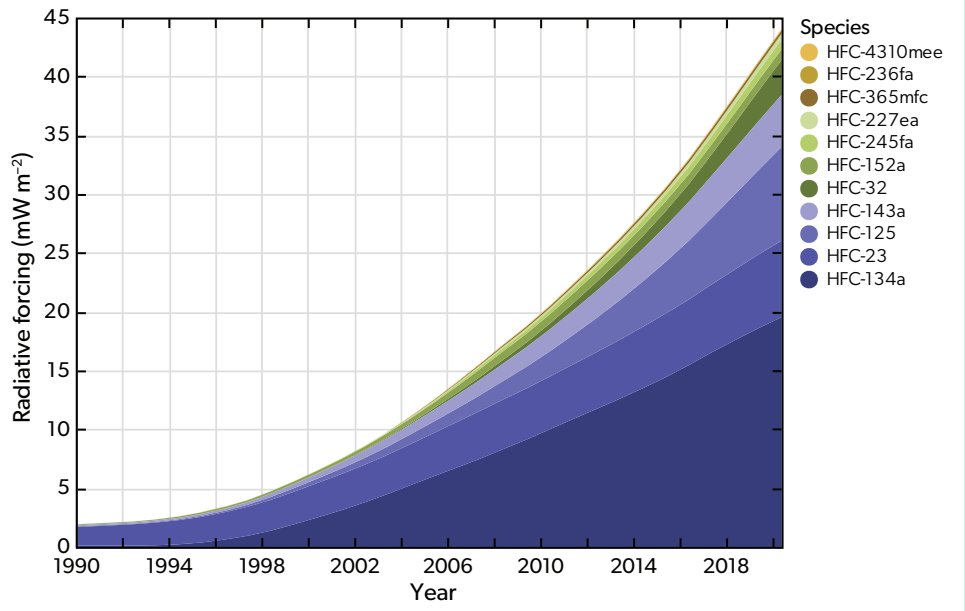

Figure 2-9. Radiative forcing due to HFCs derived from AGAGE mole fractions and the radiative efficiencies given in the *Annex*.

presented in the previous Assessment (Montzka, Velders et al., 2018). Both were substantially lower than the emissions from the bottom-up studies of Fang et al. (2016, 2018) (**Figure 2-4**). Top-down Chinese HFC-152a emissions were found to be relatively stable at ~5 Gg yr^{-1} (~10% of global emissions) during the 2011–2017 period (Yao et al., 2019). Based on measurements from an aircraft campaign in June and July 2016, Say et al. (2019) estimate that HFC-152a emissions from India were 1.2 (0.9–1.4) Gg yr^{-1}, contributing around 2% to global emissions.

2.2.1.5 HFC-245fa ($CHF_2CH_2CF_3$), HFC-365mfc ($CH_3CF_2CH_2CF_3$), HFC-227ea (CF_3CHFCF_3), HFC-236fa ($CF_3CH_2CF_3$)

HFC-245fa, HFC-365mfc, HFC-227ea, and HFC-236fa are present in the atmosphere at lower abundances than the above species (<5 ppt in 2020). Correspondingly, they have relatively small radiative forcings, making between the 6th and 11th most important contributions to overall HFC radiative forcing. Their lifetimes span a wide range, from 7.9 (HFC-245fa) to 213 years (HFC-236fa), and 100-year GWPs range from 969 (HFC-365mfc) to 9120 (HFC-236fa) (*Annex*). HFC-245fa and HFC-365mfc are used primarily as blowing agents replacing HCFC-141b and others in the production of foam products (**Table 2-1**). HFC-227ea is used as a fire suppressant, primarily replacing halon-1211 in streaming applications and halon-1301 in total flooding situations. HFC-227ea is also used with HFC-134a as a propellant in metered dose inhalers and, with HFC-365mfc, in foam blowing to reduce flammability. HFC-236fa is used in niche refrigeration applications.

The abundances of all four compounds have grown since the previous Assessment, reaching 3.2 ± 0.3 ppt (HFC-245fa; AGAGE data), 1.1 ± 0.2 ppt (HFC-365mfc; AGAGE and NOAA), 1.8 ± 0.1 ppt (HFC-227ea; AGAGE and NOAA) and 0.20 ± 0.04 ppt (HFC-236fa; AGAGE) in 2020 (**Figure 2-1** and **Table 2-2**). The growth of HFC-245fa, HFC-227ea, and HFC-236fa is roughly consistent with the projections of Velders et al. (2015), but the projected growth of HFC-365mfc was higher than has been observed. Together, these species contributed 1.6 mW m^{-2} to radiative forcing of climate in 2020.

Global emissions derived from atmospheric observations in the background atmosphere have increased since the previous Assessment for HFC-245fa, HFC-227ea, and HFC-236fa, while those of HFC-365mfc may have decreased slightly. Emissions in 2020 were 13.7 ± 2.3 Gg yr^{-1} (HFC-245fa; AGAGE), 6.1 ± 0.6 Gg yr^{-1} (HFC-227ea; AGAGE and NOAA), 3.9 ± 0.9 Gg yr^{-1} (HFC-365mfc; AGAGE and NOAA), and 0.39 ± 0.09 Gg yr^{-1} (HFC-236fa; AGAGE). The sum of the 2020 emissions of these four compounds was equivalent to approximately 42 Tg CO_2-eq yr^{-1}.

Emissions reported to the UNFCCC represented only a fraction of the global top-down estimates for each of these compounds. For HFC-245fa, HFC-227ea, HFC-365mfc, and HFC-236fa, Annex I reports represented 27%, 23%, 51%, and 37% of their global top-down total, respectively. However, as noted in the previous Assessment, much of this discrepancy likely stems from the fact that many countries report these species aggregated with others as an "unspecified mix" without sufficient information to disaggregate the mix.

Regional estimates of emissions from China, the UK, and Australia have become available since the last Assessment (Montzka, Velders et al., 2018). For China, top-down estimates were about 10–40% of the global total for these HFCs in 2017 (Yao et al., 2019; **Figure 2-4**). For HFC-245fa, the top-down values were substantially higher than the bottom-up estimates of Li et al. (2019) and Fang et al. (2018). For HFC-227ea, the top-down values were between the two bottom-up studies, and for HFC-236fa, they were similar to the bottom-up estimates of Li et al. (2019). (Fang et al., 2018, estimated zero emissions of HFC-236fa until the end of the study period in 2014.) Top-down Australian emissions estimates account for less than 2% of the global total in 2016 for all four compounds (Dunse et al., 2018). Similarly, top-down UK emissions estimates of HFC-227ea were around 1% of the global top-down value in 2018 (Manning et al., 2021). The UK

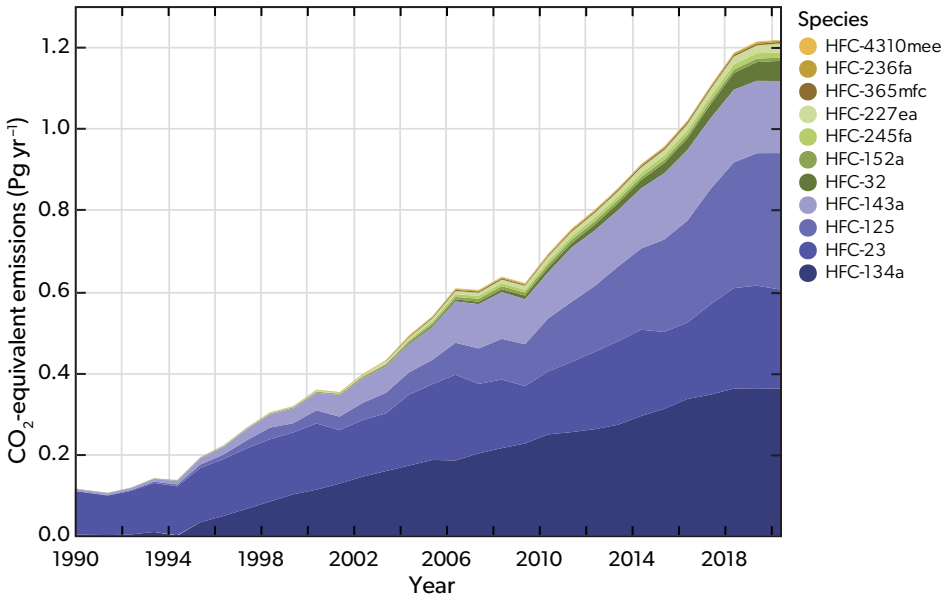

Figure 2-10. CO_2-equivalent emissions of the HFCs, as derived from AGAGE and NOAA concentration data and the 100-year GWPs from **Table 2-1** and in the *Annex*.

top-down emissions were around half of those reported by the UK to the UNFCCC.

2.2.1.6 HFC-43-10mee ($CF_3CHFCHFCF_2CF_3$)

HFC-43-10mee is the 10th-largest contributor to HFC radiative forcing, with a lifetime of 17 years and a 100-year GWP of 1610. It is used as a solvent in electronics and precision cleaning, replacing CFC-113 and methyl chloroform (**Table 2-1**). Its abundance in the atmosphere continues to increase, growing by 0.03 ± 0.03 ppt (13 ± 12%) between 2016 and 2020 and reaching 0.30 ± 0.02 ppt in 2020 (AGAGE data, **Table 2-2** and **Figure 2-1**). The radiative forcing due to HFC-43-10mee in 2020 was 0.11 ± 0.01 mW m^{-2}. Emissions derived from observed concentrations at remote AGAGE stations have not changed significantly since 2016 and were 1.2 ± 0.3 Gg yr^{-1} in 2020 (**Figure 2-2**), about 80 times higher than the most recent bottom-up UNFCCC reports. The 2020 emissions were equivalent to 1.9 ± 0.5 Tg CO_2-eq yr^{-1}.

2.2.2 Summed Radiative Forcing and CO_2-eq Emissions for HFCs

The summed radiative forcing due to the HFCs has increased by around one-third (11.0 ± 0.7 mW m^{-2}) since the previous Assessment, reaching 44.1 ± 0.6 mW m^{-2} in 2020 (**Figure 2-9**; AGAGE data). HFC-134a accounts for around 44% of this total, with the next-largest contributions coming from HFC-125 (18%), HFC-23 (15%), and HFC-143a (10%). Since the previous Assessment, radiative forcing due to HFC-125 has overtaken that of HFC-23. The radiative forcing due to the HFCs was around 13% that of the ODSs in 2020 (*Chapter 1*) and approximately 2% of that of CO_2 (https://gml.noaa.gov/aggi/aggi.html).

Total CO_2-eq emissions due to the HFCs were 1.22 ± 0.05 Pg CO_2-eq yr^{-1} in 2020, 19% higher than in 2016 (**Figure 2-10**). Of this total, HFC-134a was responsible for approximately 30%, HFC-125 for 28%, HFC-23 for 20%, and HFC-143a for 15%. The remaining species contributed less than 5% each. Chapter 2 of the last Assessment (Montzka, Velders et al., 2018) noted that GWP-weighted emissions from HFCs, HCFCs, and CFCs were similar in 2016. In 2020, because of the continuing decline in CFC and HCFC emissions and the growth of HFCs, CO_2-equivalent total emissions due to HFCs were 60–70% higher than those of CFCs or HCFCs (see *Chapter 1*).

2.2.3 Aggregate Emissions of HFCs Reported to the UNFCCC and Contributions from Non-reporting Countries

In the above subsections, the gap between top-down emissions and those reported to the UNFCCC is described for each species. For all the HFCs for which UNFCCC reports are available, this gap has grown since the previous Assessment (except for HFC-365mfc, for which the gap slightly declined). When considered in aggregate CO_2-eq emissions, the 2019 UNFCCC reports explain 31% (including HFC-23) or 37% (excluding HFC-23) of the top-down global total, down from 38% or 45% in 2015, respectively (**Figure 2-11**).

The cause of the gap between UNFCCC reports and global top-down emissions estimates is not well understood. The gap is likely dominated by emissions from non-Annex I countries, which are not required to report emissions to the UNFCCC. As also described in the previous Assessment and above, regional inverse modeling studies have not found evidence of underreporting of aggregate HFC emissions from Europe, the USA, or Australia (e.g., Lunt et al., 2015; Hu et al., 2017; Schoenenberger et al., 2019; Manning et al., 2021; Dunse et al., 2018). The measurement network used to infer top-down emissions is not sensitive to all reporting countries, but because the USA and Europe accounted for approximately three-quarters of total reported Annex I emissions in 2019, it is unlikely that underreporting in the remaining Annex I countries can account for a substantial fraction of the overall emissions gap. For non-Annex I countries, top-down emissions by Yao et al. (2019) suggest that, excluding HFC-23, around 21% of the 2017 gap (and 25% of the 2016 gap) could be explained by emissions from China (**Figure 2-11**). Top-down

emissions from India (Say et al., 2019) suggest that around 9% of the 2016 gap (both excluding or including HFC-23) could be explained by emissions from India, although there may be large uncertainty in this estimate, as it is based on a single aircraft sampling campaign that took place over a limited time period (approximately two months) and did not sample air representative of emissions from the entire country. Total emissions from South Africa in 2017, for HFC-125 and HFC-152a only, contribute less than 1% of the gap (Kuyper et al., 2019). For 2016, the year with emissions estimates for both China and India, the origin of around 40% of global CO_2-equivalent HFC emissions remained unaccounted for by UNFCCC reporting and atmospheric measurement-based regional emissions estimates (excluding HFC-23, for which top-down estimates are not available for China). These emissions likely originate primarily from non-Annex I countries where a lack of inventory reporting and sparse or non-existent atmospheric sampling preclude the robust quantification of regional emissions.

2.2.4 Next-Generation Substitutes

Unsaturated HFCs, known as hydrofluoroolefins (HFOs), have been increasingly used as lower-GWP alternatives to saturated HFCs or in blends with high-GWP HFCs. Although these compounds have GWPs similar to that of CO_2 (*Annex*), their atmospheric lifetimes are on the order of days (*Annex*), much shorter than saturated HFCs. These species are not subject to the controls of the Kigali Amendment to the Montreal Protocol.

To the best of our knowledge, there are no comprehensive global datasets on the production and consumption of HFOs. However, some atmospheric observations indicate growing regional emissions. Vollmer et al. (2015) reported atmospheric measurements of HFO-1234yf and HFO-1234ze(E) at an urban (Dubendorf) and a remote (Jungfraujoch) site in Switzerland. They also reported on measurements of the unsaturated HCFC (hydrochlorofluoroolefin) HCFO-1233zd(E) (see *Chapter 1*). Here, the Jungfraujoch measurements are updated through 2020 (**Figure 2-12**). The measurements show that the background atmospheric abundances of both compounds in central Europe have continued to grow, from less than 0.01 ppt before 2016 to annual median levels of 0.10 and 0.14 ppt for HFO-1234yf and HFO-1234ze(E), respectively, in 2020.

2.3 ATMOSPHERIC CHEMISTRY OF HFCs

2.3.1 Update on Kinetics and Lifetimes

HFCs are removed from the atmosphere primarily by reaction with the hydroxyl radical (OH) in the troposphere. Reaction with electronically excited atomic oxygen ($O(^1D)$) and OH in the stratosphere also contributes to the loss of long-lived HFCs and impacts their lifetimes slightly. Other loss processes include photolysis at the Lyman-α wavelength (mainly 121.6 nm) and dissolution into the ocean. The photochemical degradation at the Lyman-α wavelength is applicable to extremely long-lived species that can reach the mesosphere, and the oceanic loss is applicable only to a few soluble species, such as HFC-134a, HFC-125, and HFC-23 (Yvon-Lewis and Butler, 2002). Both processes have negligible impacts on total atmospheric lifetime of HFCs and therefore are not considered in the lifetime calculation. A comprehensive list of atmospheric lifetimes of HFCs, as well as HFOs, can be found in the *Annex*. The best-estimate lifetimes for major HFCs remain unchanged since the last Assessment.

2.3.2 Chemical Reactions and Impact on Atmospheric Composition

Following OH-initiated destruction of HFCs and HFOs in the atmosphere, carbon dioxide (CO_2) and hydrogen fluoride (HF) are the major stable breakdown products. Some of these

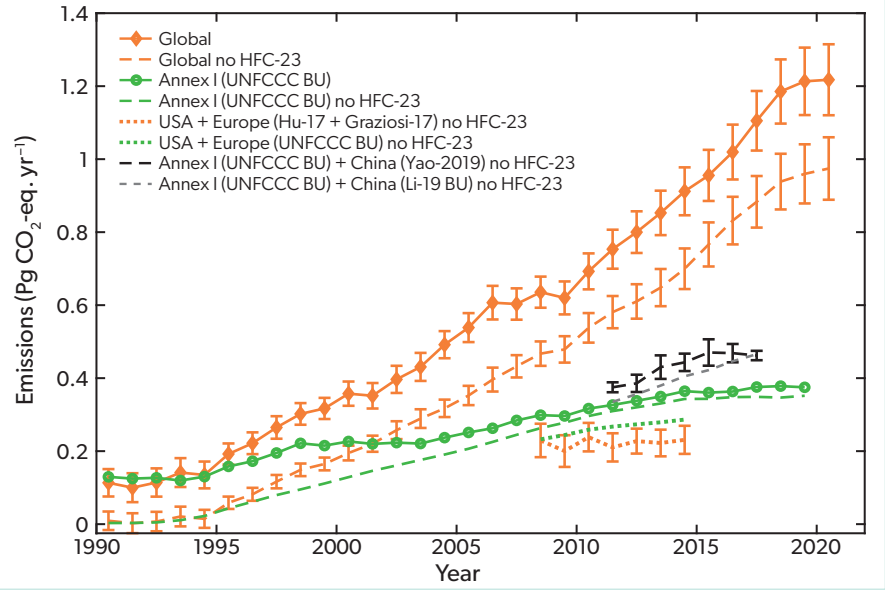

Figure 2-11. Summed CO_2-eq emissions from top-down estimates compared to those using UNFCCC reported emissions. Global aggregated HFC emissions derived from AGAGE and NOAA data are shown as the orange lines (solid, including HFC-23; dashed, excluding HFC-23). Emissions reported by Annex I countries to the UNFCCC are shown as the green lines (solid, including HFC-23; dashed, excluding HFC-23). Summed reported HFC emissions for the USA and Europe (excluding HFC-23) are shown as the dotted green line, and top-down estimate for the same regions are shown as the orange dotted line (Graziosi et al., 2017; Hu et al., 2017). The sum of the UNFCCC reported emissions (excluding HFC-23) and top-down (Yao et al., 2019) or bottom-up (Li et al., 2019) emissions from China are shown as black dashed or gray dashed lines, respectively. Error bars represent 1-sigma uncertainties.

fluorocarbons also produce trifluoroacetic acid (TFA; CF_3COOH), trifluoroacetaldehyde (CF_3CHO), and, potentially, HFC-23 as products.

2.3.2.1 Trifluoroacetic Acid (TFA, CF_3COOH) Formation

Some HFCs, as well HCFCs, HFOs, and HCFOs, degrade in the atmosphere to produce TFA. TFA abundance and its environmental impacts have been assessed in many previous Assessments (e.g., Montzka, Reimann et al., 2011; Montzka, Velders et al., 2018; Carpenter, Daniel et al., 2018). Previous Assessments concluded that the environmental effects of TFA due to the breakdown of HCFCs and HFCs are too small to be a risk to the environment over the next few decades based on the projected future use of hydrocarbons, HCFCs, and HFOs. However, they also recommended that environmental effects of TFA produced from these gases be reevaluated regularly because their emissions are increasing and sources and sinks of TFA are uncertain (Montzka, Reimann et al., 2011; Montzka, Velders et al., 2018; Carpenter, Daniel et al., 2018).

HFOs that have atmospheric lifetimes on the order of days are used as lower-GWP alternatives to the long-lived HFCs (lifetime >1 year, see *Annex*). In particular, HFO-1234yf has been increasingly used as an HFC-134a replacement refrigerant in mobile air conditioners (MAC). If the same amount of short-lived HFOs were used as replacement for the long-lived HFCs, their atmospheric breakdown would occur at a much faster rate and at locations much closer to where they were emitted. As a result, the deposition of TFA formed from degradation of these compounds would be much larger over a shorter time frame and become more localized. In this section, we assess the impact of this transition from HCFCs and long-lived HFCs to short-lived HFOs and focus on the HFC-134a to HFO-1234yf transition and how this affects TFA abundance. Projected future global production of TFA and its deposition rate related to projected HFC-134a and HFO-1234yf emissions for 2020–2100 are presented in *Chapter 7*.

TFA is highly soluble and is scavenged from the atmosphere via rain, fog, and snow, as well as dry deposition. Some fraction of the TFA dissolved in cloud water can partition back into the gas phase when the cloud water evaporates. More than 90% of TFA is physically removed from the atmosphere via wet and dry deposition (about 80% via wet deposition and 10% via dry deposition; Holland et al., 2021), with an estimated global mean deposition lifetime of about 5–10 days (Hurley et al., 2004; Holland et al., 2021). TFA is also chemically destroyed in the atmosphere by OH. This is estimated to be a minor loss channel (about 6%; Holland et al., 2021), with a global mean partial lifetime against OH of ~4 months (Chiappero et al., 2006). Criegee intermediate chemistry, under which ozone reacts with biogenic emissions of alkenes (Chhantyal-Pun et al., 2017), is a minor contribution to overall global TFA loss (<1%) but is important near the surface in the forested regions where biogenic emissions are high (Holland et al., 2021). Once in contact with soil or surface water, TFA reacts with minerals to form salt. TFA in salt form is extremely stable and persistent in the hydrosphere, with a hydrospheric half-life of centuries or greater (Solomon et al., 2016), so it accumulates in lakes and the ocean.

TFA is present ubiquitously in the hydrosphere in small concentrations. In surface freshwater, TFA levels are typically 10–300 ng L^{-1} (Carpenter, Daniel et al., 2018). TFA in freshwater is most likely a result of industrialization, as no detectable level (<2–5 ng L^{-1}) of TFA was found in very old groundwater or in preindustrial freshwater samples (Berg et al., 2000; Nielsen et al., 2001). This is consistent with the findings from ice core samples (Pickard et al., 2020), where deposition of TFA to the Arctic environment was essentially absent until the 1970s and increased substantially after the onset of HFC-134a production and emissions. New rainwater TFA concentration measurements have been reported for Germany (Freeling et al., 2020). During a nationwide 12-month field monitoring campaign in Germany, the mean TFA concentration was 703 ng L^{-1} in 1187 collected and analysed precipitation samples (Freeling et al., 2020). TFA enters the environment directly and indirectly through industrial uses. It is manufactured as an industrial chemical and is widely used. It can also be formed during the breakdown of many ODSs and ODS substitutes that contain a CF_3 group (Solomon et al., 2016). Molar yields of TFA are estimated to be 100% for HFC-1234yf (Burkholder et al., 2015; Lindley et al., 2019) and HCFC-124 (Burkholder et al., 2015), 7–20% for HFC-134a (Wallington et al., 1994), and 60% for HCFC-133a (Burkholder et al., 2015). TFA is also formed from CF_3CHO, another degradation product of some HFCs, HFOs, and HCFOs (Chiappero et al., 2006). Formation of TFA from CF_3CHO can also occur in the aqueous phase. Research shows that about 20–33% of CF_3CHO will enter the water phase and is quickly hydrated (Rayne and Forest, 2016). A recent study suggests that after remobilization into the gas phase, hydrated aldehydes in cloud droplets can be converted to organic acids by reaction with OH radicals (Franco et al., 2021). This mechanism can potentially convert hydrated CF_3CHO to form TFA. For the time being, no global modeling study is available that fully accounts for all processes in the contribution of CF_3CHO to TFA formation.

TFA is present in the ocean even at great depths and in remote locations (Frank et al., 2002; Solomon et al., 2016; UNEP 2014). The reported consistent concentration of TFA at around 200 ng L^{-1} regardless of location or depth, down to the deepest parts of ocean (Frank et al., 2002), suggests small but ubiquitous natural sources in seawater. In contrast, Scott et al. (2005) found parts of the oceans that contained very little TFA, less than 10 ng L^{-1}. However, it is unclear how representative these measurements are for the global abundance of TFA in seawater. A comprehensive review of published TFA measurements in preindustrial and other environmental examples pointed out that there were limited analytical details and uncertainties in these earlier measurements (Joudan et al., 2021). As more sources of TFA are being identified and new plausible mechanisms are proposed that can potentially transport TFA into the deep ocean on decadal timescales or faster, the presence of TFA in the deep ocean may not provide sufficient evidence that TFA occurs naturally (Joudan et al., 2021).

Since the previous Assessment, there have been new global 3-D chemical transport modeling studies to assess TFA formation in hypothetical scenarios in which refrigerants in all MACs in existence today were assumed to contain solely HFO-1234yf. These studies estimated TFA formation and deposition in the USA, Europe, China, India, and the Middle East (Wang et al., 2018; David et al., 2021). In these studies, the global total deposition of TFA produced from HFO-1234yf degradation was estimated to be approximately 60 Gg yr^{-1}. The model-simulated annual total TFA deposition rates were 7.5 Gg yr^{-1} in the USA (Wang et al.,

2018), 5.9 Gg yr^{-1} in the EU (Wang et al., 2018), 19–24 Gg yr^{-1} in China (Wang et al., 2018; David et al., 2021), 12–21 Gg yr^{-1} in India (David et al., 2021), and 10–19 Gg yr^{-1} in the Middle East (David et al., 2021). The simulated TFA rainwater concentrations show large variation, but the regional mean concentrations were below the "no observable effect" concentration for most of the areas around the globe, suggesting that the environmental impacts are insignificant (David et al., 2021). In some parts of North Africa and the Middle East where precipitation is scarce, simulated TFA rainwater concentrations exceeded the no-effect level for the most sensitive algae (1.2×10^5 ng L^{-1}) (Solomon et al., 2016; Wang et al., 2018). However, this finding is based on a single model study, and there are large uncertainties in model-calculated precipitation amounts and TFA rainwater concentrations in regions with very low precipitation.

In Chapter 6 of the last Assessment (Carpenter, Daniel et al., 2018), HFC-134a was estimated to make the largest contribution of the HCFCs and HFCs to TFA formation globally. Atmospheric measurements in central Europe show that the mean background molar fraction of HFC-1234yf at Jungfraujoch has increased from <1 parts per quadrillion (ppq) in 2014 (Vollmer et al., 2015) to about 0.10 ± 0.07 ppt in 2020 (**Figure 2-12**, updated from Vollmer et al., 2015). With an abundance of about 0.10 ± 0.07 ppt, an atmospheric lifetime of 14 days, and 100% TFA molar yield, the breakdown of HFC-1234yf is estimated to form a comparable, or possibly larger, amount of TFA near Jungfraujoch than from the breakdown of HFC-134a (mean background abundance of 120.7 ± 2.9 ppt at Jungfraujoch in 2020, lifetime of 14 years, 7–20% TFA molar yield). Like HFC-1234yf, the atmospheric annual mean background concentrations of HFO-1234ze(E) and HCFO-1233zd(E) at Jungfraujoch have increased rapidly in the recent years to around 0.1 ppt in 2020 (*Section 2.2.4* and *Section 1.3.1.1*). If their atmospheric levels continue to grow in the coming years, their contributions to TFA formation need to be considered in the atmospheric TFA budget estimate. Due to the limited representativeness of Jungfraujoch measurements and the large spatial variability and uncertainties related to short-lived HFOs and their atmospheric chemical loss, it is difficult to assess the contribution of HFC-1234yf, and similarly HFO-1234ze(E) and HCFO-1233zd(E), to TFA formation on a global scale. Currently, the measured and model-simulated concentrations of TFA from the use of HFOs, HFCs, HCFCs, and HCFOs for present-day conditions in general remain significantly below known toxicity limits, but continued work is needed as updates to science are made, particularly for the regions that could be vulnerable to adverse impacts in future.

The transition from use of HFCs to HFOs will lead to more TFA and less HF formation. Both are substances considered potential contributors to acidification. Lindley et al. (2019) compared the acidification potential of HFCs, HFOs and HCFOs emissions in the EU and concluded that the relative acidification potential of these compounds is very similar and that these compounds contribute less than 0.5% of the main acidification air pollutants—sulfur dioxide (SO_2), nitrogen oxides (NO_x) and ammonia (NH_3)—resulting in an insignificant contribution to acidification both presently and up to at least 2030.

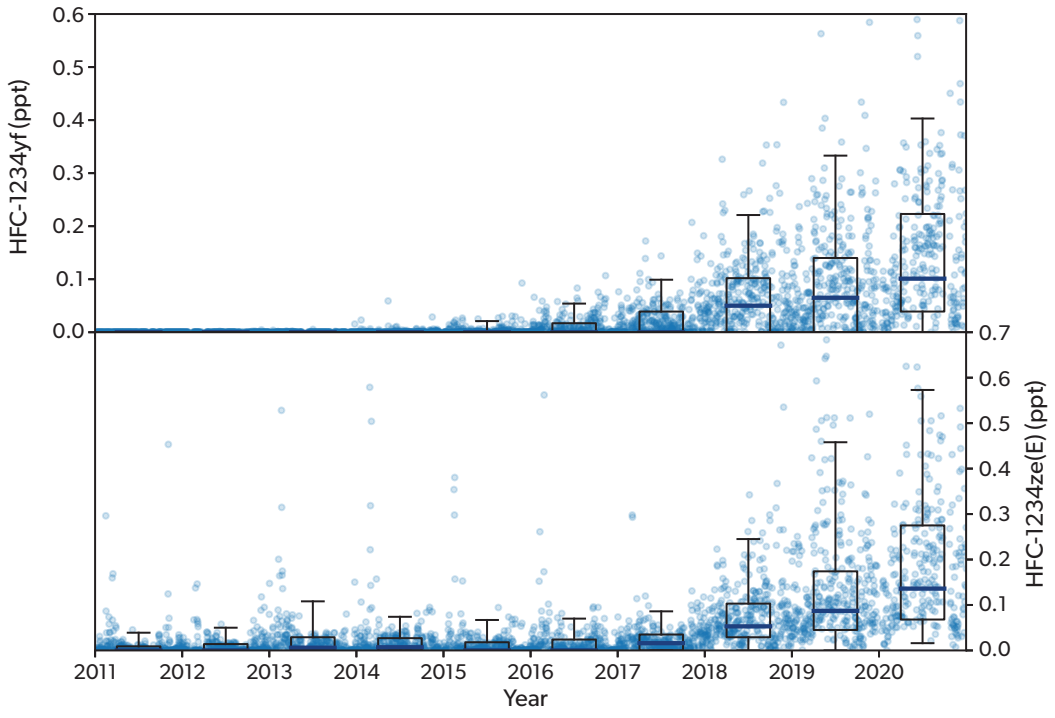

Figure 2-12. Measurements of HFO-1234yf and HFO-1234ze(E) at Jungfraujoch. Points show daily averages of data collected approximately every two hours. Boxes indicate the 25th and 75th percentiles of the two-hourly data within each year, and the whiskers show the 5th and 95th percentiles. The median is indicated by the thick gray line inside each box. [Updated from Vollmer et al., 2015.]

2.3.2.2 Trifluoroacetaldehyde (CF_3CHO) Formation and Impact

CF_3CHO is a minor degradation product of some fluorinated compounds and is linked to TFA chemistry (see above). CF_3CHO is primarily formed in the atmosphere during the degradation of HFC-143a, HFO-1234ze(E), and HCFO-1233zd(E), with a 100% CF_3CHO molar yield from each compound (Sulbaek Andersen et al., 2018; Burkholder et al., 2015). Photolysis of CF_3CHO can potentially form HFC-23 in the atmosphere (Chiappero et al., 2006; Burkholder, et al., 2015), although the significance of HFC-23 formation via this mechanism is not well quantified at present.

CF_3CHO is primarily removed from the atmosphere via photolysis, with a photolysis lifetime of a few days (Chiappero et al., 2006). Loss of CF_3CHO can also occur through reaction with OH radicals, with an OH partial lifetime of ~24 days (Scollard et al., 1993; Sellevåg et al., 2004). It has an additional minor loss mechanism by reacting with Cl radicals (Scollard et al., 1993; Burkholder, et al., 2015). CF_3CHO photolysis can proceed via three pathways at solar radiation wavelengths >290 nm (Chiappero et al., 2006; Burkholder, et al., 2015):

$$CF_3CHO + hv \longrightarrow CF_3 + HCO \quad \textit{(pathway 1)}$$
$$\longrightarrow CHF_3 + CO \quad \textit{(pathway 2)}$$
$$\longrightarrow CF_3CO + H \quad \textit{(pathway 3)}$$

Chiappero et al. (2006) reported a CF_3CHO total quantum yield of 0.17 ± 0.03 for pathway 1. The quantum yield of a photochemical reaction describes the number of molecules undergoing a photochemical event per absorbed photon. The quantum yield for pathway 2 is <0.02 at 308 nm, suggesting this is a negligible HFC-23 source (Chiappero et al., 2006). Updated photolysis experiments also found no detectable (<0.3%) production of CHF_3 during the photolysis of CF_3CHO under conditions representative of the troposphere (ambient pressures of air, N_2, or O_2 and with wavelengths ranging from 400 nm to 290–300 nm; Sulbaek Anderson and Nielsen, 2022).

Measurements at central European stations show an atmospheric mean background molar fraction of ~0.20 ppt for HFO-1234ze(E) and ~0.18 ppt for HCFO-1233zd(E) (update from Vollmer et al., 2015). Since HFO-1234ze(E) and HCFO-1233zd(E), like the long-lived HFCs, are predominantly destroyed by OH oxidation in the troposphere, with background concentrations of ~0.2 ppt (lower in more remote regions) and assuming a <0.3% CHF_3 formation rate during CF_3CHO photolysis, their contribution to HFC-23 formation in the atmosphere is negligible. With a global concentration of 25.8 ppt and a lifetime of 51 years, the contribution of HFC-143a to CF_3CHO and subsequent HFC-23 formation is also negligible.

2.3.2.3 Impact on Tropospheric Ozone

The atmospheric degradation of HFCs can contribute to tropospheric ozone formation, but their photochemical ozone creation potentials are very small (Montzka, Velders et al., 2018). There are no updates since the previous Assessment, and the impact of HFCs on tropospheric ozone formation are still estimated to be negligible. A recent modeling analysis by Sulbaek Andersen et al. (2018) assessed the impact on ozone formation of commercially relevant ODSs and HFCs replacing HFOs and HCFOs, including HCFO-1233zd, and concluded that they too will have a small impact.

2.4 POTENTIAL FUTURE CHANGES

In Chapter 2 of the previous Assessment (Montzka, Velders et al., 2018), scenarios were presented with projections of HFC consumption, emissions, and radiative forcing through 2050. These consisted of scenarios without national or international regulations on the use of HFCs (from Velders et al., 2015, and termed "baseline" scenarios in the previous Assessment) and scenarios with a phasedown of HFC production and consumption according to the 2016 Kigali Amendment to the Montreal Protocol (Montzka, Velders et al., 2018). In *Section 2.4.1* these scenarios are compared with emissions inferred from HFC observations through 2020. In *Section 2.4.2*, an updated Kigali Amendment scenario is presented based on updated consumption data, on updated emissions inferred from observations, on national policies in place in the EU, USA, and Japan, and on the phasedown schedule of the 2016 Kigali Amendment. Also presented are zero-production and zero-emissions scenarios, used to illustrate the hypothetical limit of the effects of further global policy options.

2.4.1 Comparison of WMO (2018) Scenarios with Inferred Emissions

The scenarios presented in Chapter 2 of the previous Assessment (Montzka, Velders et al., 2018) were based on HFC emissions and activity data reported to the UNFCCC up to 2011, HCFC consumption data reported to UNEP up to 2013, observations of HFC mixing ratios up to 2013, assumptions about growth in demand for HFCs, and assumptions on how much of this demand would be met by HFCs or not-in-kind alternatives (Velders et al., 2015). In **Figure 2-13**, the global CO_2-eq emissions from the 2018 scenario without control measures are compared with emissions inferred from measured global HFC concentration trends from the AGAGE and NOAA networks from 2010 to 2020. In contrast to *Section 2.2*, in this section, top-down global annual emissions were calculated using a 1-box atmospheric model, as in Velders et al. (2015), rather than the 12-box model. Because this model estimates annual emissions from the difference in mole fraction between subsequent Januarys, estimates are provided through 2019, rather than 2020. The global total HFC CO_2-eq emissions projected in the 2018 scenario without control measures exceed those derived from atmospheric observations by about 20% for the 2017–2019 period (**Figure 2-13**).

The smaller inferred emissions, compared to the 2018 scenario with no control measures, result largely from lower emissions of HFC-125 and HFC-143a (**Figure 2-14**). Top-down emissions are lower than those in the 2018 scenario without control measures for HFC-32, HFC-125, and HFC-143a: HFC-32 is 19% below the scenario averaged over 2017–2019; HFC-125, 25% below; and HFC-143a, about 40% below. The global top-down emissions of HFC-143a slowly increased up to 2015 and then were approximately constant from 2016 to 2019. HFC-143a is used mainly in the blend R-404A[2] in industrial and commercial refrigeration (ICR) applications. In the scenario without control measures, it was assumed that global consumption would increase following the growing demand for refrigeration applications, mainly in

[2] R404A is a blend, by mass, of 44% HFC-125, 52% HFC-143a, and 4% HFC-134a. Using the GWPs in the Kigali Amendment, it has a GWP of 3921.6.

developing countries, and the phaseout of HCFC-22 following the Montreal Protocol provisions. The fact that the global emissions of HFC-143a are significantly below the scenario and were approximately constant from 2016 to 2019 indicates that during the ongoing phaseout of HCFC-22, the ICR sector turned away from HFC-143a and employed non-HFC alternatives or switched to lower-GWP blends in larger amounts.

According to data reported to the UNFCCC (2021), the EU and USA have the largest reported use of HFC-143a of all Annex I countries (Velders et al., 2022). The use in the EU decreased by about 60% in 2017 compared to 2010. This decrease preceded the prohibition on the use of HFCs with a GWP larger than 2500 for commercial refrigeration applications, which is in effect from 2020 (EU, 2014). This is in line with a finding from TEAP (2019) that in Europe, R-404A has already been replaced by an HFC blend (R-452A[3]) without HFC-143a. In the USA, the use of HFC-143a increased by 14% in 2017 compared to 2010, and small increases are also seen in other developed countries. The net effect is that in 2017,the total Annex I use decreased by about 8% compared to 2010. Based on the decreased use of HFC-143a in developed countries and the trend in observed emissions, additional lines are added to **Figures 2-13** and **2-14** in which the 2018 scenario without control measures is adjusted for the period 2013–2020. In this adjusted scenario, the projected use of HFCs in ICR is reduced for developed countries following the UNFCCC reported reduction in HFC-143a use, and the use of HFCs in ICR in developing countries is held constant at the 2013 level. With these adjustments, the baseline emissions of HFC-143a and HFC-125 are close to the emissions inferred from observations (**Figure 2-14**). The adjusted emissions scenario ("Reduced HFC use in ICR" in **Figures 2-13** and **2-14**) more closely follow the emissions inferred from observations (NOAA and AGAGE in **Figures 2-13** and **2-14**).

2.4.2 Scenario Based on National Policies and the Kigali Amendment

An updated HFC scenario is constructed for the period 2019–2050, which takes into account updated trends in consumption and emissions, national regulations in place by 1 January 2021, and the provisions of the Kigali Amendment. The national regulations include the EU F-gas regulation (EU, 2014) and MAC directive (EU, 2006), the HFC phasedown in the USA (US EPA, 2021a), and regulations in Japan (METI, 2015). This scenario uses the same procedure as the baseline scenario in Velders et al. (2015).

The updated 2022 Kigali Amendment scenario starts with a consumption scenario without any national regulation or international protocols, after which the national regulations are applied, followed by the provisions of the Kigali Amendment. The scenario is based on detailed information reported by Annex I countries to the UNFCCC (2021) for individual HFCs per use sector from 1990 to 2018, HCFC consumption data from 1989 to 2019 reported by non-A5 and A5 countries to UNEP (2021), and observations of HFC mixing ratios up to 2020. In addition, data are used from historical HFC consumption in China for 1995–2017 derived from Chinese statistical data (Li et al., 2019) and HFC emissions of India for 2016 estimated from observed mixing ratios (Say et al., 2019).

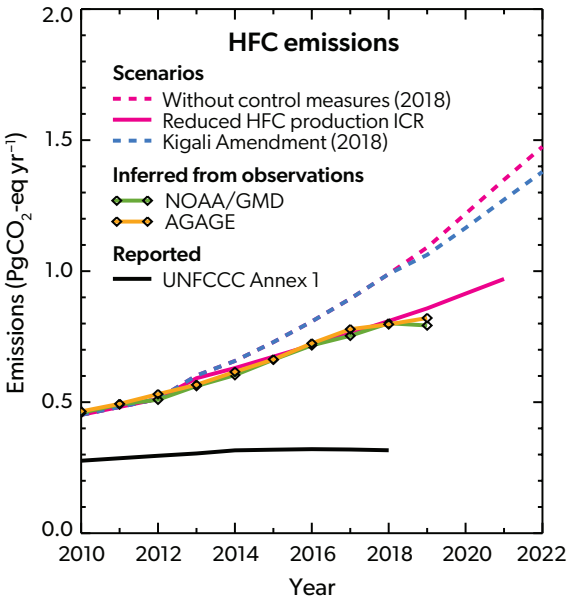

Figure 2-13. Global average HFC emissions ($PgCO_2$-eq yr^{-1}) from the WMO (2018) scenario without control measures (previously called the "baseline" scenario in Montzka, Velders et al., 2018, originating from Velders et al., 2015), from the 2018 Kigali Amendment scenario (Montzka, Velders et al., 2018), and from emissions inferred from observed mixing ratios from the AGAGE and NOAA networks. The solid red line shows an adjusted scenario with reduced HFC production for industrial and commercial refrigeration (ICR) from 2013 onward. The 2018 scenarios were constrained by the emissions inferred from observed mixing ratios up to 2013. Also shown are the emissions reported to the UNFCCC by Annex I countries. The curves contain the sum of all HFC emissions except HFC-23. [Figure from Velders et al., 2022.]

An upper and lower range of this scenario is constructed using the same assumptions for growth in demand for HFCs and not-in-kind alternatives in non-A5 and A5 countries as for the baseline scenarios from the previous Assessment (Velders et al., 2015; Montzka, Velders et al., 2018; Velders et al., 2022). As such, the demand in A5 countries grows proportionally with gross domestic product, and the demand in non-A5 countries grows proportional to the growth in population. Assumptions (see Velders et al., 2015) about how much of this demand was met by HFCs or not-in-kind alternatives follow those in the previous Assessment, except for the use of HFCs for ICR applications because the trends in observed mixing ratios indicate smaller use of HFCs in this sector (*Section 2.4.1*). Therefore, for A5 countries, the use of HFCs for ICR in the lower range is kept constant at the 2018 level. In non-A5 countries, the use of HFCs for ICR grows only slightly, following growth in population, as in the scenario without control measures of WMO (2018). The growth in some sectors might be underestimated in the scenarios when they are driven by new

[3] R-452A is a blend, by mass, of 11% HFC-32, 59% HFC-125, and 30% HFO-1234yf. Using the GWPs in the Kigali Amendment, it has a GWP of 2139.25.

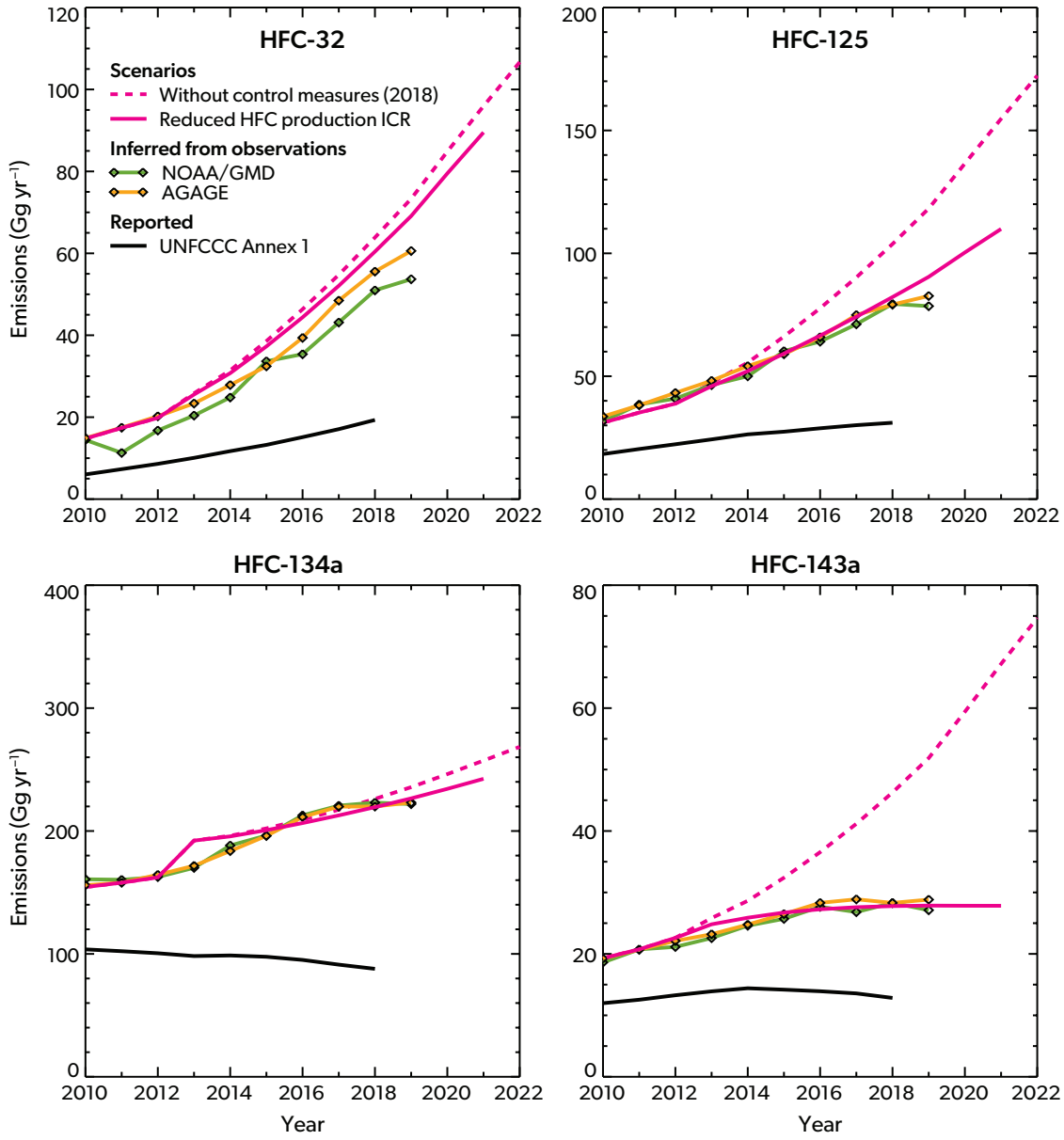

Figure 2-14. Global average HFC emissions (Gg yr^{-1}) from the 2018 scenario without control measures (previously called the "baseline" scenario) compared with emissions inferred from observed mixing ratios from the AGAGE and NOAA networks. The solid red line shows an adjusted scenario with reduced HFC production for industrial and commercial refrigeration (ICR) from 2013 onward. Also shown are the emissions reported to the UNFCCC by Annex I countries. The scenarios were constrained by the emissions inferred from observed mixing ratios up to 2013. [Figure from Velders et al., 2022.]

and strongly growing markets. An example could be heat pumps that replace gas boilers for heating buildings. See Velders et al. (2022) for details of the scenarios.

The policies already in place in the EU, USA, and Japan are applied to the scenario limiting the production and consumption in these (groups of) countries. The provisions of the 2016 Kigali Amendment are then applied. Any HFC consumption in excess of the limits of the national policies or the Kigali Amendment is assumed to be replaced by low-GWP alternative substances or alternative technologies.

The Kigali Amendment (2022 update) scenario is shown in **Figures 2-15** and **2-16**. The regional and sectoral contributions to HFC CO_2-eq emissions for the upper range of the scenario are shown in **Figure 2-15**, while the contributions of the different HFCs to global emissions by mass and weighted by their GWP in the upper range of the Kigali Amendment scenario are shown in **Figure 2-16**. The largest 2050 contributions are projected to be from China and other A5 countries. Stationary air-conditioning

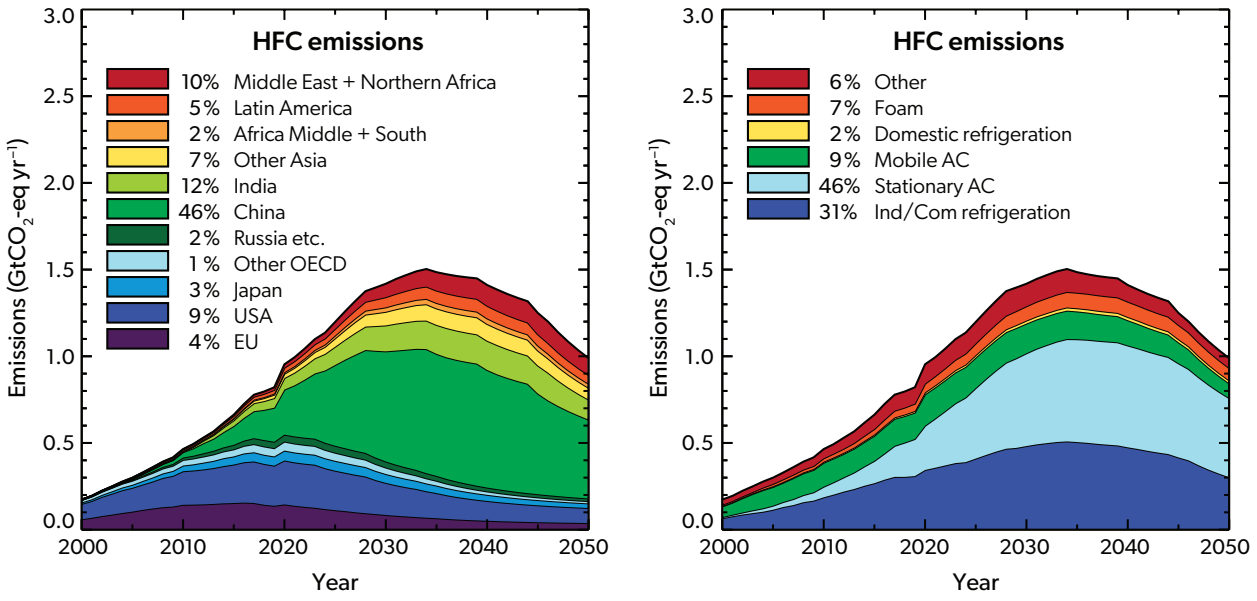

Figure 2-15. Contributions of the HFCs in 11 regions *(left)* and 6 use sectors *(right)* to the CO_2-eq emissions from the 2022 Kigali Amendment scenario based on updated observations and reported consumption, national policies, and the provisions of the Kigali Amendment (upper-range scenario). The percentages in the legend refer to the relative contributions in 2050. The regions are the EU and UK, USA, Japan, other Organization for Economic Co-operation and Development (OECD) countries, states of the former Soviet Republics (Russia) and Yugoslavia, China, India, other Asian countries, central and southern Africa, Latin America, and the Middle East plus Northern Africa. The use sectors are: 1) industrial, commercial (open compressor), commercial (hermetically sealed compressor), and transport refrigeration; 2) stationary air-conditioning; 3) mobile air-conditioning; 4) domestic refrigeration; 5) foams (extruded polystyrene, polyurethane, and open cell foams); and 6) other (aerosol products, fire extinguishing systems, and solvents). The data before 2020 are partly based on observed mixing ratios, while from 2020 to 2050 the data are based on the 2022 Kigali Amendment scenario, which causes some discontinuity around 2020. Contributions from HFC-23 are not included. The CO_2-eq emissions shown here are based on the GWPs from WMO (2018). Scenarios are from Velders et al. (2022).

and ICR are projected to give the largest sector contributions. The difference between the upper and lower ranges of these scenarios is small compared to that of the scenario without control measures.

Emissions from the Kigali Amendment (2022 update) scenario, assuming global adoption, are projected to be 0.9–1.0 Pg CO_2-eq yr^{-1} in 2050, compared to 4.0–5.3 Pg CO_2-eq yr^{-1} from the 2018 scenario without control measures (**Figure 2-17**). The corresponding radiative forcing in the 2018 "without control measures" scenario of 0.22–0.25 W m^{-2} is reduced to 0.09–0.10 W m^{-2} in 2050 under the Kigali Amendment (2022 update) scenario. The updated projections of the emissions and radiative forcing are lower than the Kigali Amendment scenario presented in the 2018 Assessment. Compared to that scenario, the 2020–2050 cumulative emissions are reduced by 14–18 Pg CO_2-eq and the 2050 radiative forcing is reduced by 0.03 W m^{-2}. In scenarios with a cessation in global production or emissions of HFCs in 2023, the projected emissions and radiative forcing are further reduced. If production of HFCs were to cease in 2023, the radiative forcing would be reduced to about 0.03 W m^{-2} in 2050, and would decline thereafter. Cumulative 2020–2050 emissions would be reduced by 21–26 Pg CO_2-eq relative to the Kigali Amendment (2022 update) scenario. If all emissions (from new production and from banks) ceased in 2023, radiative forcing due to HFCs would decline to 0.01 W m^{-2} by 2050, with cumulative emissions being reduced by 32–37 Pg CO_2-eq relative to the updated Kigali Amendment scenario (**Figure 2-17**). These scenarios are not necessarily achievable, but they provide useful information on the lower limits of future radiative forcing due to HFCs.

2.4.2.1 HFC-23 Scenarios

Unlike other HFCs, which have a phasedown schedule that extends over several decades, the Kigali Amendment mandates that "Each country manufacturing HCFC-22 or HFCs shall ensure that starting in 2020 the emissions of HFC-23 generated in production facilities are destroyed to the extent practicable using technology approved by the Montreal Protocol" (UNEP, 2016). Without abatement, HFC-23 emissions were projected to increase to ~20 Gg yr^{-1} by 2016 and ~24 Gg yr^{-1} by 2035 (Miller and Kuijpers, 2011). Emissions for 2020, derived from atmospheric observations, were 16.5 ± 0.9 Gg yr^{-1}, below the worst-case scenario in Miller and Kuijpers (2011) but above the best-practice scenario, which was 0 Gg yr^{-1} in 2020 (and substantially higher than bottom-up estimates based on recent abatement reports; *Section 2.2.1.2*).

As outlined in *Section 2.2.1.2*, *Chapter 7*, and Stanley et al. (2020), only a minor quantity of the theoretical possible

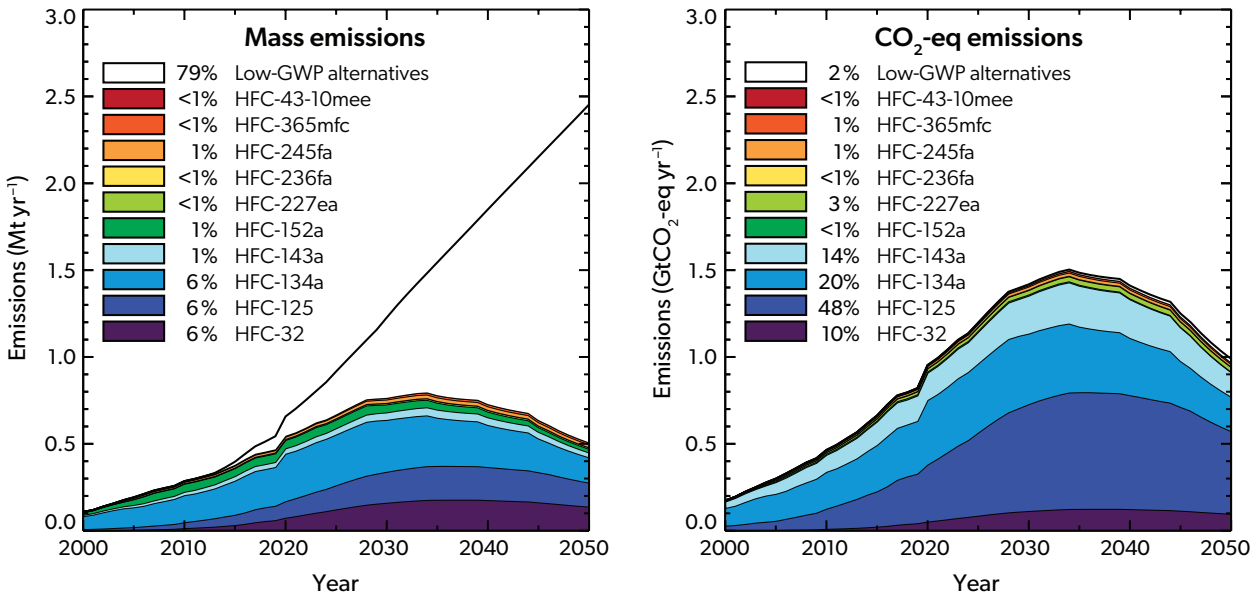

Figure 2-16. Contributions of the different HFCs to global emissions (in Tg yr^{-1} and Pg CO_2-eq yr^{-1}) from the 2022 Kigali Amendment scenario based on updated observations and reported consumption, national policies, and the provisions of the Kigali Amendment (upper-range scenario). Also shown are the contributions from alternative substances and/or technologies used to replace HFCs, indicated as "low-GWP alternative." The percentages refer to the relative contributions in 2050. The CO_2-eq emissions shown here are based on the GWPs from WMO (2018). [Adapted from Velders et al., 2022.]

abatement capacity seems to have been realised in the most recent years. Two different scenarios have been developed in *Chapter 7* to project future HFC-23 emissions within this Assessment. Both scenarios are outlined in *Section 7.2.2.1* and assume similar increases in HCFC-22 production. The first scenario assumes the widespread use of abatement such that emissions of HFC-23 are only 0.08% relative to the produced HCFC-22 (97% effective destruction capacity of HFC-23 by-product plus small emissions related to failures and maintenance of destruction systems). The second scenario assumes business-as-usual behavior (1.8% emissions relative to HCFC-22 production), where destruction capacities are only partly exploited.

Under the business-as-usual scenario, if the current fractional rate of HFC-23 destruction continues into the future, radiative forcing due to HFC-23 is expected to reach 0.015 W m^{-2} in 2050. Under the scenario in which there is widespread destruction of HFC-23 by-product, the contribution of HFC-23 to overall HFC radiative forcing will be small (*Section 7.2.2.1*).

2.4.3 Surface Temperature Contributions from HFCs

Radiative forcing contributes to global surface warming, changes in atmospheric circulation, sea level rise, and other warming-related climate changes. The contribution of HFCs (**Figure 2-17**) to surface warming is shown in **Figure 2-18**. For this calculation, the scenarios are extended to 2100, based on the same assumptions as used for 2020–2050. In the new scenario following current trends, national policies, and the provisions of the Kigali Amendment, the HFCs are projected to contribute 0.04°C to the global average surface warming in 2100, compared to 0.3–0.5°C in the baseline scenarios of the previous Assessment (Montzka, Velders et al., 2018; Velders et al., 2022). The updated Kigali Amendment scenario leads to a temperature rise that is slightly lower than that of the previous Assessment. For comparison, all greenhouse gases (GHGs) are projected to contribute 1.4–4.4°C to surface warming by the end of the 21st century, following the IPCC scenarios (best estimate for 2081–2100; IPCC, 2021). In hypothetical scenarios with a cease in global production or emissions of HFCs in 2023, the contribution to surface warming is reduced to no more than 0.01°C in 2100.

2.4.4 New and Expanding Uses of HFCs

Since the previous Assessment, HFC use may have expanded to similar uses or into a higher percentage of markets where competing non-HFC technologies exist. Most of the HFC uses and emissions continue to come from end uses that traditionally used ODSs. In this section, we briefly describe several technologies that traditionally did not rely on ODSs.

There is a growth in use of HFCs in vapor-compression cycles for air and/or water heating. Devices that use this process, for both cooling and heating, have been used for several decades and have typically been referred to as "heat pumps." This same terminology is also used to refer to newer equipment types that are designed to provide heating and that are often not reversible to provide cooling. In space heating, e.g., for occupant comfort, such heat pumps typically replace boilers or electric resistance heating. In addition to the potential gains in energy efficiency, the use of heat pumps will decarbonize (except for any HFC leakage) the heating at the building or central plant site, although the emissions from the power supply need to be considered in any full life-cycle analysis.

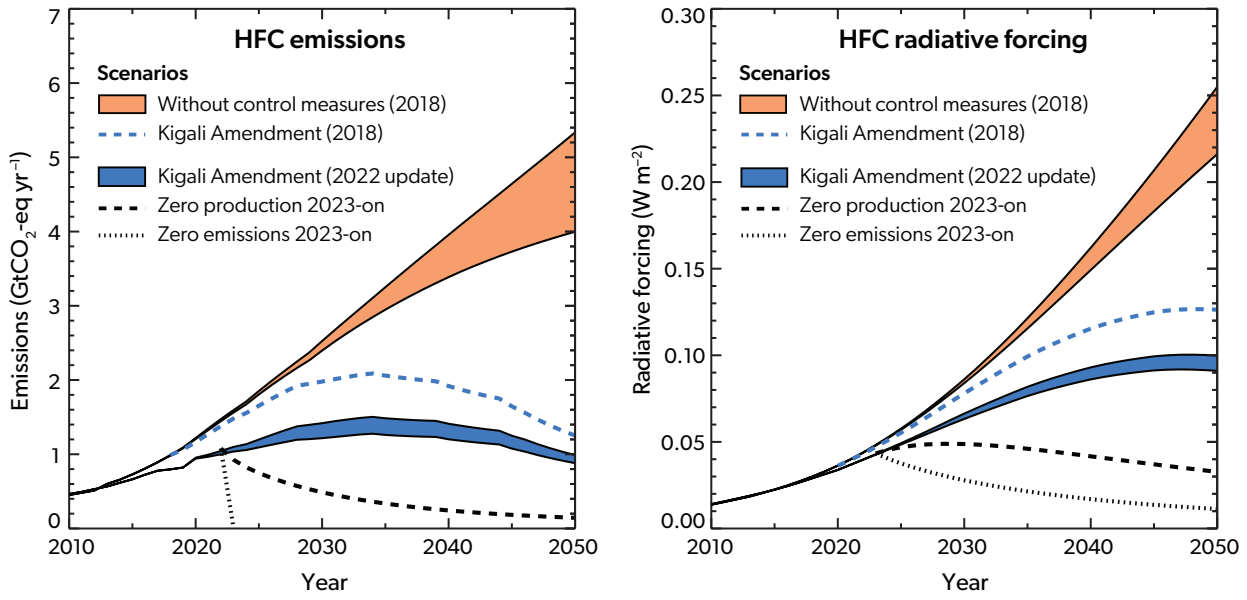

Figure 2-17. Global average HFC emissions (Pg CO_2-eq yr^{-1}) (*left*) and radiative forcing *(right)* ranges from the 2018 scenario without control measures (Montzka and Velders et al., 2018, based on Velders et al., 2015; orange) and on scenarios based on updated observations and reported consumption, national policies, and the Kigali Amendment provisions (blue shading). Also shown is a scenario that follows the phasedown schedules of the Kigali Amendment from the 2018 Assessment (blue dashed lines). Scenarios in which the global HFC production ceases in 2023 or the global HFC emissions cease in 2023 are given in black dashed and dotted lines, respectively. The data shown use the lifetimes, GWPs, and radiative efficiencies from WMO (2018). The curves contain the contributions of all HFCs except HFC-23 (see *Sections 2.4.2.1* and *7.2.2.1*). Scenarios from Velders et al. (2022).

For water heating, a heat pump provides hot, potable water that can be supplied for typical uses (showers, dish washing, laundry, etc.), utilized in radiator systems for space heating, or used in a combination system that performs both functions. R-410A[4] and HFC-134a dominate the market for these types of technologies (UNEP, 2018c). National and regional HFC controls may cause the market to shift to lower-GWP refrigerants if reductions in other sectors do not adequately provide the reductions necessary to allow for the increase in this use.

Heat pump technology has also been introduced as an energy-efficient option for clothes drying, replacing the typical tumble dryer that uses electric resistance heating. HFC-134a is the primary refrigerant used; models using R-407C[5] and R-290 (propane) are also available. R-450A[6] has also been used (EFTC, 2021). The primary market for these units has been in non-A5 countries (UNEP, 2018c).

There may be additional use of HFC cooling in electric vehicles, for passenger comfort and to provide cooling to the electric battery (UNEP, 2018c). In some instances, two separate systems are employed for the two functions; in others, a heat pump is used for both. These systems require refrigerant charges 30–50% higher than mobile air-conditioning in internal combustion engine vehicles. With the growing number of electric vehicles, this would lead to an increased use of high-GWP HFCs (e.g., HFC-134a) if such systems are not transitioned to low-GWP alternatives (e.g., HFO-1234yf or carbon dioxide [CO_2]).

HFC-134a is used as a solvent for the extraction of oil from dry biomass. This is currently applied in the cannabis oil industry (Timatic, 2021a), which is seen as a growing market due to the increase in the legalization of marijuana use. The same process has also been applied to the production of a large range of aromatic and flavoring agents, such as chocolate, cinnamon, lemon peels, and vanilla bean (Costello, 2021; MMV, 2006).

HFCs have been used in small quantities in other applications that did not previously rely on ODSs. In magnesium production and processing, there is minor use and emissions of HFC-134a as part of a proprietary blend sold under the trade name AM-cover™. This option and others (CO_2, FK-5-1-12) replace the high-GWP cover gas typically used—sulfur hexafluoride (SF_6) mixed with dry air and/or CO_2. HFC emissions from this source are small, for example, amounting to 0.1 Tg CO_2-eq yr^{-1} in the USA for the past five years (US EPA, 2021b).

Other potential applications—such as cork poppers, desk ornaments (such as dunking birds), and airsoft pistols—use minimal amounts of HFCs, having generally shifted to other alternatives

[4] R-410A is a blend, by mass, of 50% HFC-32 and 50% HFC-125. Using the GWPs in the Kigali Amendment, it has a GWP of 2087.5.
[5] R-407C is a blend, by mass, of 23% HFC-32, 25% HFC-125, and 52% HFC-134a. Using the GWPs in the Kigali Amendment, it has a GWP of 1773.85.
[6] R-450A is a blend, by mass, of 42% HFC-134a and 58% HFO-1234ze(E). Using the GWPs in the Kigali Amendment, it has a GWP of 600.6.

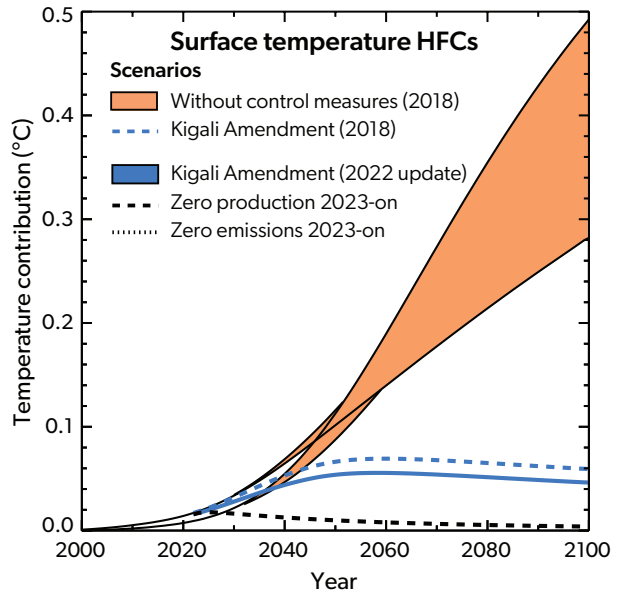

Figure 2-18. Contribution of HFCs to the global average surface warming for the 2018 scenarios without control measures (orange) and for the updated 2022 Kigali Amendment scenario based on updated observations and reported consumption, national regulations, and the Kigali Amendment provisions (solid blue line). The scenarios without control measures are from the previous Assessment and are based on Xu et al. (2013) and Velders et al. (2015). Also shown are the effects of the provisions of the Kigali Amendment presented in the 2018 Assessment (dashed blue line) and scenarios assuming that the global production or emissions of HFCs would cease in 2023 (dashed black line). No range is shown for the updated 2022 Kigali Amendment since the lower and upper range scenarios virtually coincide. The surface temperature change for the Kigali Amendment scenarios is calculated using the MAGICC6 model. Lifetimes, GWPs, and radiative efficiencies are taken from WMO (2018). The curves contain the contributions of all HFCs except HFC-23 (see *Sections 2.4.2.1* and *7.2.2.1*). [Adapted from Velders et al., 2022.]

including argon, dichloromethane (CH_2Cl_2; also known as methylene chloride), and propane, respectively.

2.4.5 Alternatives to High-GWP HFCs

The mandate to phase down high-GWP HFCs has triggered a major effort to find and implement more environmentally benign alternatives. HFOs and blends that contain HFOs were identified as the most promising replacements (McLinden et al., 2020). For example, in non-A5 countries, HFO-1234yf is now used in most new automotive air-conditioning systems as a replacement for HFC-134a, and it is expected to be used universally in the coming years in the EU, USA, and Japan. HFO-1234ze(E) and HFO-1336mzz(Z) have been used as foam-blowing agents and as refrigerants in chillers. Other HFOs that are being developed include HFO-1132a as a feedstock for fluoropolymers and HFO-1123 as a replacement for R-410A, by blending it with HFC-32. Many of these are slightly flammable, presenting trade-offs between safety and environmental considerations. None of the HFOs are a direct replacement for R-410A. Instead, non-flammable blends—which often contain some combination of HFO-1234yf, HFO-1234ze(E), HFC-32, HFC-134a, and HFC-125—have been proposed to replace R-410A (Kujak and Schultz, 2019). HFC-32 is also used as a single-component refrigerant replacement for R-410A in some equipment.

Nonfluorinated refrigerants, primarily ammonia, carbon dioxide, propane, and isobutane, are seeing renewed interest as alternatives to ODSs and HFCs in a wide range of applications and may have contributed to the slower-than-projected rise in emissions from 2013–2020 (**Figure 2-13**). These refrigerants all have zero ozone depletion potential (ODP) and very low global warming potential (GWP) compared to fluorinated refrigerants, making them environmentally attractive possibilities. Ammonia is considered to be a superior refrigerant because of its thermodynamic properties, and application is relatively easy in large, low-temperature systems (McLinden et al., 2020). However, due to its toxicity and flammability, ammonia may not be appropriate in some systems. Carbon dioxide is being used across a wide range of systems such as supermarkets, ice rinks, heat pump water heaters, data center cooling, automotive air-conditioning, and industrial freezers (McLinden et al., 2020). However, engineering CO_2-based systems to be efficient, especially in warmer climates, requires them to be very complex compared to traditional equipment, which also makes them more expensive to construct and maintain. Hydrocarbons are used for refrigeration in oil refineries, where the flammability hazard of a hydrocarbon refrigerant is readily addressed, as well as in very small systems such as domestic refrigerators. Based on research findings, safety standards are changing, allowing larger amounts of hydrocarbons in additional equipment types.

2.4.6 Energy Efficiency

As discussed in Chapter 2 of the last Assessment (Montzka, Velders et al., 2018), the climate impact of the expanding base of air-conditioning and refrigeration equipment will depend on several factors. These can be divided into a "direct effect" from refrigerant leakage (unless a zero-GWP refrigerant is used) and an "indirect effect" resulting from the production and transmission of energy (generally, electricity) to operate the product. The indirect effect is highly variable depending on the local energy supply, which changes as different energy sources are deployed over the day and throughout the seasons. It is important to understand the assumptions used when assessing the GHG emissions reduction potential from energy efficiency improvements, because such emissions reduction benefits may decrease in the future as the energy supply is decarbonized.

Changing the refrigerant alone would not drive significant energy efficiency improvements compared to the equipment used today (UNEP, 2018d). Depending on the equipment or system in use with a high-GWP refrigerant, UNEP (2018d) expected only about ±10% change in energy efficiency from switching to a low-GWP refrigerant (i.e., without concurrent changes to the equipment). However, the transition to new refrigerants provides

an opportunity to implement energy-efficient design changes. Such change could lead to energy efficiencies, compared to current equipment, in the range of 10–70% (UNEP, 2018d). UNEP (2020d) found that highly energy-efficient products using low-GWP alternatives are available, but accessibility to these technologies is low in many A5 countries and in some non-A5 countries. Looking at the situation in seven A5 countries, four non-A5 countries, and Europe as a whole, the study found that the market average energy efficiency was typically far below the best energy efficiency available in each country (or region).

TEAP (2021) reviewed and summarized several studies of the potential benefits of phasing down high-GWP HFCs while improving equipment efficiency. TEAP has reported that technology has developed rapidly, and there is now availability of refrigeration and air conditioning equipment with enhanced energy efficiency and lower GWP refrigerants in all sectors covered in its report. These technologies are increasingly accessible worldwide. Peters (2018) analyzed the growth of cooling equipment (space cooling, stationary refrigeration, and mobile cooling), finding that under a "current technology progress" scenario, energy use alone would lead to emissions of 7.4 Pg CO_2-eq yr^{-1} by 2050. With no assumptions of refrigerant changes, this scenario found an additional 1.5 Pg CO_2-eq yr^{-1} from refrigerant emissions. In a "cooling for all" scenario (i.e., high proliferation of air-conditioning in regions that experience high temperatures), emissions were projected to rise to 18.8 Pg CO_2-eq yr^{-1} by 2050. With significant improvements in energy efficiency and use of low-GWP refrigerants, emissions could be limited to 13.3 Pg CO_2-eq yr^{-1} by 2050 under that scenario. UNEP and IEA (2020d) also examined the increasing demand for cooling technologies and discussed policies and financing strategies to address the consequent environmental effect, including international initiatives, implementation of minimum energy performance standards, improved building design to reduce demand, and cessation of the resale of obsolete and inefficient equipment. The report suggested that by improving energy efficiency while phasing down high-GWP HFCs in refrigeration and air-conditioning, global GHG emissions of up to 210–460 Pg CO_2-eq would be avoided over the next four decades, depending on future rates of decarbonization of the power grid.

Shah et al. (2019), Dreyfus et al. (2020), and Purohit et al. (2020) quantified the overall benefits to climate that could be achieved through the integration of lower-GWP refrigerant adoption with deployment of more efficient equipment. These studies projected benefits of similar orders of magnitude from energy efficiency improvements and from moving to lower-GWP refrigerants, assuming both policies are pursued at the same time. Projecting near-universal saturation of air-conditioning in all warm areas, Shah et al. (2019) estimated avoidance by 2050 of up to 240.1 Pg CO_2-eq in GHG emissions under efficiency improvements (of ~30%) that the authors deemed as low-cost and up to 373 Pg CO_2-eq using best-available technologies. Dreyfus et al. (2020) found similar results, estimating that widespread adoption of the best currently available technologies could reduce the climate emissions from stationary air-conditioning and refrigeration by 130–260 Pg CO_2-eq by 2050 and 210–460 Pg CO_2-eq by 2060. The energy efficiency improvements in Dreyfus's scenarios account for about 75% of the benefits seen. Purohit et al.

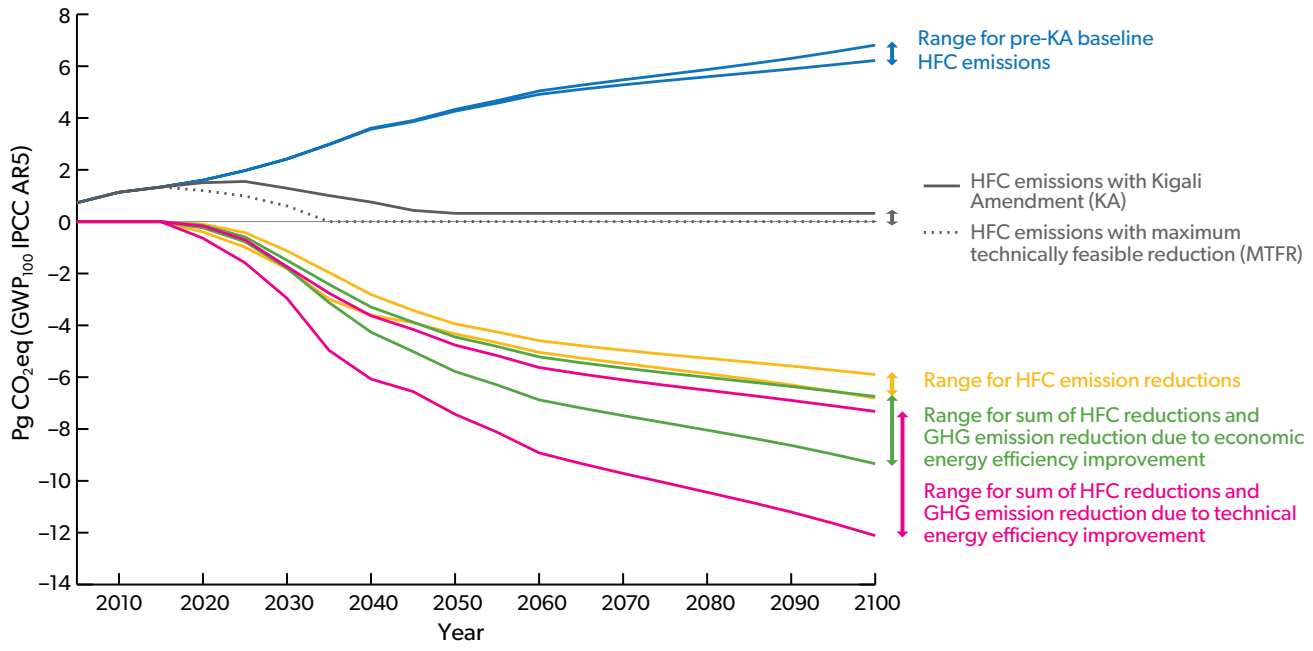

Figure 2-19. Full range of HFC CO_2-eq emissions under scenarios that either do not account for the effects of the Kigali Amendment (blue) or that do account for the Kigali Amendment and maximum technically feasible reduction scenarios (grey). Also shown are the range of mitigation potential (i.e., potential avoided emissions) (yellow) and the summed emissions benefits (Pg CO_2-eq yr^{-1}) due to HFC reductions and other greenhouse gas mitigation under technical or economic energy efficiency improvements (red and green, respectively). [Adapted from Purohit et al., 2020, Figure 7.]

(2020) incorporated a change in fuel mix (i.e., a lower CO_2-eq kWh^{-1} emissions factor from electric supply) along with an HFC phasedown and energy efficiency improvements, finding that the combination could prevent 411–631 Pg CO_2-eq emissions from stationary cooling equipment between 2018 and 2100 (**Figure 2-19**). Purohit et al. (2020) found that climate benefits from improved energy efficiency in stationary cooling technologies are about the same magnitude as those from the HFC phasedown.

REFERENCES

Barletta, B., Nissenson, P., Meinardi, S., Dabdub, D., Sherwood Rowland, F., VanCuren, R. A., Pederson, J., Diskin, G. S., Blake, D. R.. HFC-152a and HFC-134a emission estimates and characterization of CFCs, CFC replacements, and other halogenated solvents measured during the 2008 ARCTAS campaign (CARB phase) over the South Coast Air Basin of California. ***Atmospheric Chemistry and Physics***, ***11***(6), 2655–2669. https://doi.org/10.5194/acp-11-2655-2011, 2011.

Berg, M., S.R. Müller, J. Mühlemann, A. Wiedmer, and R.P. Schwarzenbach, Concentrations and mass fluxes of chloroacetic acids and trifluoroacetic acid in rain and natural waters in Switzerland, ***Environ. Sci. Technol.***, ***34*** (13), 2675–2683, doi:10.1021/es990855f, 2000.

Bernath, P.F., J. Steffen, J. Crouse, and C.D. Boone, Sixteen-year trends in atmospheric trace gases from orbit, ***J. Quant. Spect. Rad. Trans.***, ***253***, 107178, doi:10.1016/j.jqsrt.2020.107178, 2020.

Bernath, P.F., J. Crouse, R.C. Hughes, and C.D. Boone, The Atmospheric Chemistry Experiment Fourier transform spectrometer (ACE-FTS) version 4.1 retrievals: Trends and seasonal distributions, ***J. Quant. Spect. Rad. Trans.***, ***259***, 107409, doi:10.1016/j.jqsrt.2020.107409, 2021.

Boone, C.D., P.F. Bernath, D. Cok, S.C. Jones, and J. Steffen, Version 4 retrievals for the atmospheric chemistry experiment Fourier transform spectrometer (ACE-FTS) and imagers, ***J. Quant. Spect. Rad. Trans., 247***, 106939, doi:10.1016/j.jqsrt.2020.106939, 2020.

Burkholder, J.B., S.P. Sander, J. Abbatt, J.R. Barker, R.E. Huie, C.E. Kolb, M.J. Kurylo, V.L. Orkin, D.M. Wilmouth, and P.H. Wine, ***Chemical Kinetics and Photochemical Data for Use in Atmospheric Studies***, Evaluation No. 18, JPL Publication 15-10, Jet Propulsion Laboratory, National Aeronautics and Space Administration, Pasadena, California, [available at: http://jpldataeval.jpl.nasa.gov], 2015.

Carpenter, L.J., and J.S. Daniel (Lead Authors), E.L. Fleming, T. Hanaoka, J. Hu, A.R. Ravishankara, M.N. Ross, S. Tilmes, T.J. Wallington, and D.J. Wuebbles, Scenarios and Information for Policymakers, Chapter 6 in ***Scientific Assessment of Ozone Depletion: 2018***, Global Ozone Research and Monitoring Project–Report No. 58, World Meteorological Organization, Geneva, Switzerland, 2018.

Chiappero, M.S., F.E. Malanca, G.A. Argüello, S.T. Wooldridge, M.D. Hurley, J.C. Ball, T.J. Wallington, R.L. Waterland, and R.C. Buck, Atmospheric chemistry of perfluoroaldehydes ($C_xF_{2x+1}CHO$) and fluorotelomer aldehydes ($C_xF_{2x+1}CH_2CHO$): Quantification of the important role of photolysis, ***J. Phys. Chem. A***, ***110*** (43), 11,944–11,953, doi:10.1021/jp064262k, 2006.

Chhantyal-Pun, R., M. R. McGillen, J. M. Beames, M. A. H. Khan, C. J. Percival, D. E. Shallcross, A. J. Orr-Ewing, Temperature-Dependence of the Rates of Reaction of Trifluoroacetic Acid with Criegee Intermediates, ***Angew. Chem. Int. Ed.***, 56, 9044, doi:10.1002/anie.201703700, 2017.

Costello, ***Advanced Pytonics Extraction Technology using HFC-134a***, Costello, [available at: https://rccostello.com/extraction.html], 2021.

Cunnold, D.M., R.G. Prinn, R.A. Rasmussen, P.G. Simmonds, F.N. Alyea, C.A. Cardelino, A.J. Crawford, P.J. Fraser, and R.D. Rosen, The atmospheric lifetime experiment: 3. Lifetime methodology and application to three years of CFCl3 data, ***J. Geophys. Res., 88*** (C13), 8379–8400, doi:10.1029/Jc088ic13p08379, 1983.

David, L.M., M. Barth, L. Höglund-Isaksson, P. Purohit, G.J.M. Velders, S. Glaser, and A.R. Ravishankara, Trifluoroacetic acid deposition from emissions of HFO-1234yf in India, China, and the Middle East, ***Atmos. Chem. Phys.***, ***21*** (19), 14,833–14,849, doi:10.5194/acp-21-14833-2021, 2021.

Dreyfus, G., N. Borgford-Parnell, J. Christensen, D.W. Fahey, B. Motherway, T. Peters, R. Picolotti, N. Shah, and Y. Xu, ***Assessment of Climate and Development Benefits of Efficient and Climate-Friendly Cooling***, Climate & Clean Air Coalition and Institute for Governance & Sustainable Development, Molina, M., and D. Zaelke (Steering Committee co-chairs), [available at: https://ccacoalition.org/en/resources/assessment-climate-and-development-benefits-efficient-and-climate-friendly-cooling], 2020.

Dunse, B.L., N. Derek, P.J. Fraser, P.B. Krummel, and L.P. Steele, ***Australian and global HFC, PFC, sulfur hexafluoride nitrogen trifluoride and sulfuryl fluoride emissions***, Report prepared for Australian Government Department of the Environment and Energy, CSIRO Oceans and Atmosphere, Aspendale, Australia, iv, 33 pp., [available at: http://www.environment.gov.au/protection/ozone/publications/csiro-report-australian-global-sgg], 2018.

Ebnesajjad, S., Preparation of Tetrafluoroethylene and Other Monomers, In: ***Fluoroplastics (2nd Edition)***, William Andrew Publishing, Oxford, 48–75 pp., 2015.

EFTC (European Fluorocarbon Technical Committee), ***Heat Pumps***, [available at: https://www.fluorocarbons.org/applications/heat-pumps/], 2021.

EU (European Union), Directive 2006/40/EC of the European parliament and of the council of 17 May 2006 relating to emissions from air-conditioning systems in motor vehicles. Official J. EU L161, 12-18, [available at: https://eur-lex.europa.eu/legal-content/EN/TXT/?uri=CELEX%3A32006L0040], 2006.

EU (European Union), Regulation (EU) No 517/2014 of the European Parliament and of the Council of 16 April 2014 on fluorinated greenhouse gases and repealing Regulation (EC) No 842/2006 Text with EEA relevance, ***Off. J. Eur. Union***, ***150***, 195–230, [available at: http://data.europa.eu/eli/reg/2014/517/oj], 2014.

Fang, X., G.J.M. Velders, A.R. Ravishankara, M.J. Molina, J. Hu, and R.G. Prinn, Hydrofluorocarbons (HFCs) emissions in China: an inventory for 2005–2013 and projections to 2050, ***Environ. Sci. Technol.***, ***50*** (4), 2027–2034, doi:10.1021/acs.est.5b04376, 2016.

Fang, X., A.R. Ravishankara, G.J.M. Velders, M.J. Molina, S. Su, J. Zhang, J. Hu, and R.G. Prinn, Changes in emissions of ozone-depleting substances from China due to implementation of the Montreal Protocol, ***Environ. Sci. Technol.***, ***52*** (19), 11,359–11,366, doi:10.1021/acs.est.8b01280, 2018.

Fernando, A.M., P.F. Bernath, and C.D. Boone, Trends in atmospheric HFC-23 (CHF3) and HFC-134a abundances, ***J. Quant. Spectrosc. Radiat. Transf.***, ***238***, 106540, doi:10.1016/j.jqsrt.2019.06.019, 2019.

Franco, B., T. Blumenstock, C. Cho, L. Clarisse, C. Clerbaux, P.-F. Coheur, M. De Mazière, I. De Smedt, H.-P. Dorn, T. Emmerichs, H. Fuchs, G. Gkatzelis, D. W. T. Griffith, S. Gromov, J. W. Hannigan, F. Hase, T. Hohaus, N. Jones, A. Kerkweg, A. Kiendler-Scharr, E. Lutsch, E. Mahieu, A. Novelli, I. Ortega, C. Paton-Walsh, M. Pommier, A. Pozzer, D. Reimer, S. Rosanka, R. Sander, M. Schneider, K. Strong, R. Tillmann, M. Van Roozendael, L. Vereecken, C. Vigouroux, A. Wahner, and D. Taraborrelli, Ubiquitous atmospheric production of organic acids mediated by cloud droplets, ***Nature, 593*** (7858), 233–237, doi:10.1038/s41586-021-03462-x, 2021.

Frank, H., E.H. Christoph, O. Holm-Hansen, and J.L. Bullister, Trifluoroacetate in ocean waters, ***Environ. Sci. Technol.***, ***36*** (1), 12–15, doi:10.1021/es0101532, 2002.

Freeling, F., D. Behringer, F. Heydel, M. Scheurer, T.A. Ternes, and K. Nödler, Trifluoroacetate in precipitation: deriving a benchmark data set, ***Environ. Sci. Technol.***, ***54*** (18), 11,210–11,219, doi:10.1021/acs.est.0c02910, 2020.

Forster, P., T. Storelvmo, K. Armour, W. Collins, J.-L. Dufresne, D. Frame, D.J. Lunt, T. Mauritsen, M.D. Palmer, M. Watanabe, M. Wild, and H. Zhang, The Earth's Energy Budget, Climate Feedbacks, and Climate Sensitivity, Chapter 7 in ***Climate Change 2021: The Physical Science Basis, Contribution of Working Group I to the Sixth Assessment Report of the Intergovernmental Panel on Climate Change***, edited by V. Masson-Delmotte, P. Zhai, A. Pirani, S.L. Connors, C. Péan, S. Berger, N. Caud, Y. Chen, L. Goldfarb, M.I. Gomis, M. Huang, K. Leitzell, E. Lonnoy, J.B.R. Matthews, T.K. Maycock, T. Waterfield, O. Yelekçi, R. Yu, and B. Zhou, Cambridge University Press, Cambridge, United Kingdom and New York, NY, USA, 131 pp., doi:10.1017/9781009157896.009, 2021.

Fortems-Cheiney, A., M. Saunois, I. Pison, F. Chevallier, P. Bousquet, C. Cressot, S.A. Montzka, P.J. Fraser, M.K. Vollmer, P.G. Simmonds, D. Young, S. O'Doherty, R.F. Weiss, F. Artuso, B. Barletta, D.R. Blake, S. Li, C. Lunder, B.R. Miller, S. Park, R. Prinn, T. Saito, L.P. Steele, and Y.C.J. Yokouchi, Increase in HFC-134a emissions in response to the success of the Montreal Protocol, ***J. Geophys. Res. Atmos.***, ***120*** (22), 11,728–11,742, doi:10.1002/2015jd023741, 2015.

Graziosi, F., J. Arduini, F. Furlani, U. Giostra, P. Cristofanelli, X. Fang, O. Hermanssen, C. Lunder, G. Maenhout, S. O'Doherty, S. Reimann, N. Schmidbauer, M.K. Vollmer, D. Young, and M. Maione, European emissions of the powerful greenhouse gases

hydrofluorocarbons inferred from atmospheric measurements and their comparison with annual national reports to UNFCCC, ***Atmos. Environ.***, ***158***, 85–97, doi:10.1016/j.atmosenv.2017.03.029, 2017.

Harrison, J.J., M.P. Chipperfield, C.D. Boone, S.S. Dhomse, and P.F. Bernath, Fifteen years of HFC-134a satellite observations: comparisons with SLIMCAT calculations, ***J. Geophys. Res.***, ***126*** (8), e2020JD033208, doi:10.1029/2020jd033208, 2021.

Höglund-Isaksson, L., A. Gómez-Sanabria, Z. Klimont, P. Rafaj, and W. Schöpp, Technical potentials and costs for reducing global anthropogenic methane emissions in the 2050 timeframe–results from the GAINS model, ***Environ. Res. Commun.***, ***2*** (2), 025004, doi:10.1088/2515-7620/ab7457, 2020.

Holland, R., M.A.H. Khan, I. Driscoll, R. Chhantyal-Pun, R.G. Derwent, C.A. Taatjes, A.J. Orr-Ewing, C.J. Percival, and D.E. Shallcross, Investigation of the production of trifluoroacetic acid from two halocarbons, HFC-134a and HFO-1234yf and its fates using a global three-dimensional chemical transport model, ***ACS Earth Space Chem.***, ***5*** (4), 849–857, doi:10.1021/acsearthspacechem.0c00355, 2021.

Hu, L., S.A. Montzka, S.J. Lehman, D.S. Godwin, B.R. Miller, A.E. Andrews, K. Thoning, J.B. Miller, C. Sweeney, C. Siso, J.W. Elkins, B.D. Hall, D.J. Mondeel, D. Nance, T. Nehrkorn, M. Mountain, M.L. Fischer, S.C. Biraud, H. Chen, and P.P. Tans, Considerable contribution of the Montreal Protocol to declining greenhouse gas emissions from the United States, ***Geophys. Res. Lett.***, ***44*** (15), 8075–8083, doi:10.1002/2017GL074388, 2017.

Hurley, M.D., M.P. Sulbaek Andersen, T.J. Wallington, D.A. Ellis, J.W. Martin, and S.A. Mabury, Atmospheric chemistry of perfluorinated carboxylic acids: reaction with OH radicals and atmospheric lifetimes, ***J. Phys. Chem. A***, ***108*** (4), 615–620, doi:10.1021/jp036343b, 2004.

IPCC, Changing State of the Climate System, in Climate Change 2021: The Physical Science Basis. Contribution of Working Group I to the Sixth Assessment Report of the Intergovernmental Panel on Climate Change, edited by V. Masson-Delmotte, P. Zhai, A. Pirani, S. L. Connors, C. Péan, S. Berger, N. Caud, Y. Chen, L. Goldfarb, M. I. Gomis, M. Huang, K. Leitzell, E. Lonnoy, J. B. R. Matthews, T. K. Maycock, T. Waterfield, O. Yelekçi, R. Yu and B. Zhou (eds.), Cambridge University Press., 2021.

Joudan, S., A.O. De Silva, and C.J. Young, Insufficient evidence for the existence of natural trifluoroacetic acid, ***Environ. Sci. Process. Impacts***, ***23*** (11), 1641–1649, doi:10.1039/d1em00306b, 2021.

Kujak, S., and K. Schultz, Examination of a novel R410A replacement, ***ASHRAE Trans.***, ***125*** (2), 264–272, [available at: https://link.gale.com/apps/doc/A616448773/AONE?u=anon~8471483c&sid=googleScholar&xid=f29cece1], 2019.

Kuyper, B., D. Say, C. Labuschagne, T. Lesch, W.R. Joubert, D. Martin, D. Young, M.A.H. Khan, M. Rigby, A.L. Ganesan, M.F. Lunt, C. O'Dowd, A.J. Manning, S. O'Doherty, M.T. Davies-Coleman, and D.E. Shallcross, Atmospheric HCFC-22, HFC-125, and HFC-152a at Cape Point, South Africa, ***Environ. Sci. Technol.***, ***53*** (15), 8967–8975, doi:10.1021/acs.est.9b01612, 2019.

Laube, J.C., P. Martinerie, E. Witrant, T. Blunier, J. Schwander, C.A.M. Brenninkmeijer, T.J. Schuck, M. Bolder, T. Röckmann, C. van der Veen, H. Bönisch, A. Engel, G.P. Mills, M.J. Newland, D.E. Oram, C.E. Reeves, and W.T. Sturges, Accelerating growth of HFC-227ea (1,1,1,2,3,3,3-heptafluoropropane) in the atmosphere, ***Atmos. Chem. Phys.***, ***10*** (13), 5903–5910, doi:10.5194/acp-10-5903-2010, 2010.

Leedham Elvidge, E., H. Bönisch, C.A.M. Brenninkmeijer, A. Engel, P.J. Fraser, E. Gallacher, R. Langenfelds, J. Mühle, D.E. Oram, E.A. Ray, A.R. Ridley, T. Röckmann, W.T. Sturges, R.F. Weiss, and J.C. Laube, Evaluation of stratospheric age of air from CF_4, C_2F_6, C_3F_8, CHF_3, HFC-125, HFC-227ea and SF_6; implications for the calculations of halocarbon lifetimes, fractional release factors and ozone depletion potentials, ***Atmos. Chem. Phys.***, ***18*** (5), 3369–3385, doi:10.5194/acp-18-3369-2018, 2018.

Li, Y.X., Z.Y. Zhang, M.D. An, D. Gao, L.Y. Yi, and J.X. Hu, The estimated schedule and mitigation potential for hydrofluorocarbons phase-down in China, ***Adv. Clim. Chang. Res.***, ***10*** (3), 174–180, doi:10.1016/j.accre.2019.10.002, 2019.

Lindley, A., A. McCulloch, and T. Vink, Contribution of hydrofluorocarbons (HFCs) and hydrofluoro-Olefins (HFOs) atmospheric breakdown products to acidification ("Acid Rain") in the EU at present and in the future, ***Open J. Air Pollut.***, ***8*** (4), 81–95, doi:10.4236/ojap.2019.84004, 2019.

Lunt, M.F., M. Rigby, A.L. Ganesan, A.J. Manning, R.G. Prinn, S. O'Doherty, J. Mühle, C.M. Harth, P.K. Salameh, T. Arnold, R.F. Weiss, T. Saito, Y. Yokouchi, P.B. Krummel, L.P. Steele, P.J. Fraser, S. Li, S. Park, S. Reimann, M.K. Vollmer, C. Lunder, O. Hermansen, N. Schmidbauer, M. Maione, J. Arduini, D. Young, and P.G. Simmonds, Reconciling reported and unreported HFC emissions with atmospheric observations, ***Proc. Natl. Acad. Sci.***, ***112*** (19), 5927–5931, doi:10.1073/pnas.1420247112, 2015.

Manning, A.J., A.L. Redington, D. Say, S. O'Doherty, D. Young, P.G. Simmonds, M.K. Vollmer, J. Mühle, J. Arduini, G. Spain, A. Wisher, M. Maione, T.J. Schuck, K. Stanley, S. Reimann, A. Engel, P.B. Krummel, P.J. Fraser, C.M. Harth, P.K. Salameh, R.F. Weiss, R. Gluckman, P.N. Brown, J.D. Watterson, and T. Arnold, Evidence of a recent decline in UK emissions of hydrofluorocarbons determined by the InTEM inverse model and atmospheric measurements, ***Atmos. Chem. Phys.***, ***21*** (16), 12,739–12,755, doi:10.5194/acp-21-12739-2021, 2021.

McLinden, M.O., C.J. Seeton, and A. Pearson, New refrigerants and system configurations for vapor-compression refrigeration, ***Science***, ***370*** (6518), 791–796, doi:10.1126/science.abe3692, 2020.

MEFCC (Ministry of Environment, Forest and Climate Change), ***Control of Emission/Venting of Hydrofluorocarbon (HFC)-23, Produced as By-product While Manufacturing of Hydrochlorofluorocarbon (HCFC)-22, in the Atmosphere***, Ministry of Environment, Forest and Climate Change, New Dehli, India, [available at: http://ozonecell.nic.in/wp-content/uploads/2018/09/1482401969634-ORDER-13-OCTOBER-2016.pdf], 2016.

METI, Act on the rational use and proper management of fluorocarbons (Act no. 64 of 2001), Ministry of Economy, Trade and Industry, Japan, Tokyo., [available at: http://conf.montreal-protocol.org/meeting/workshops/hfc_management/presentations/Statements by Heads of Delegations/4-Masafumi Ohki_session_4.ppt], 2015.

Miller, B.R., M. Rigby, L.J.M. Kuijpers, P.B. Krummel, L.P. Steele, M. Leist, P.J. Fraser, A. McCulloch, C. Harth, P. Salameh, J. Mühle, R.F. Weiss, R.G. Prinn, R.H.J. Wang, S. O'Doherty, B.R. Greally, and P.G. Simmonds, HFC-23 (CHF_3) emission trend response to HCFC-22 ($CHClF_2$) production and recent HFC-23 emission abatement measures, ***Atmos. Chem. Phys.***, ***10*** (16), 7875–7890, doi:10.5194/acp-10-7875-2010, 2010.

Miller, B.R., and L.J.M. Kuijpers, Projecting future HFC-23 emissions, ***Atmos. Chem. Phys.***, ***11*** (24), 13,259–13,267, doi:10.5194/acp-11-13259-2011, 2011.

Miller, J. B., Lehman, S. J., Montzka, S. a., Sweeney, C., Miller, B. R., Karion, A., Wolak, C., Dlugokencky, E., Southon, J., Turnbull, J. C., Tans, P. P.. Linking emissions of fossil fuel CO2 and other anthropogenic trace gases using atmospheric 14CO2. ***Journal of Geophysical Research***, ***117***(D8). https://doi.org/10.1029/2011JD017048, 2012.MMV (Medicines for Malaria Venture), ***Comparative Assessment of Technologies for Extraction of Artemisinin***, Summary report commissioned through the Malalaria Medicines Venture, 17 pp., Geneva, Switzerland, [available at: https://www.mmv.org/sites/default/files/uploads/docs/publications/8_-_1_ArtemisiaExtractionStudy_3.pdf], 2006.

Montzka, S.A., and S. Reimann, (Lead Authors), A. Engel, K. Krüger, S. O`Doherty, and W.T. Sturges, Ozone-Depleting Substances (ODSs) and Related Chemicals, Chapter 1 in ***Scientific Assessment of Ozone Depletion: 2010,*** Global Ozone Research and Monitoring Project–Report No. 52, World Meteorological Organization, Geneva, Switzerland, 2011.

Montzka, S.A., M. McFarland, S.O. Andersen, B.R. Miller, D.W. Fahey, B.D. Hall, L. Hu, C. Siso, and J.W. Elkins, Recent trends in global emissions of hydrochlorofluorocarbons and hydrofluorocarbons: Reflecting on the 2007 adjustments to the Montreal Protocol, ***J. Phys. Chem. A***, ***119*** (19), 4439–4449, doi:10.1021/jp5097376, 2015.

Montzka, S.A., and G.J.M. Velders (Lead Authors), P.B. Krummel, J. Mühle, V.L. Orkin, S. Park, N. Shah, H. Walter-Terrinoni, P. Bernath, C. Boone, L. Hu, M.J. Kurylo, E.L. Elvidge, M. Maione, B.R. Miller, S. O'Doherty, M. Rigby, I.J. Simpson, M.K. Vollmer, R.F. Weiss, L.J.M. Kuijpers, and W.T. Sturges, Hydrofluorocarbons (HFCs), Chapter 2 in ***Scientific Assessment of Ozone Depletion: 2018***, Global Ozone Research and Monitoring Project–Report No. 58, World Meteorological Organization, Geneva, Switzerland, 2018.

Nielsen, O.J., B.F. Scott, C. Spencer, T.J. Wallington, and J.C. Ball, Trifluoroacetic acid in ancient freshwater, ***Atmos. Environ.***, ***35*** (16), 2799–2801, doi:10.1016/S1352-2310(01)00148-0, 2001.

Oram, D.E., W.T. Sturges, S.A. Penkett, A. Mc-Culloch, and P.J. Fraser, Growth of fluoroform (CHF_3, HFC-23) in the background atmosphere, ***Geophys. Res. Lett.***, ***25*** (1), 35–38, doi:10.1029/97GL03483, 1998.

Oram, D.E., M.J. Ashfold, J.C. Laube, L.J. Gooch, S. Humphrey, W.T. Sturges, E. Leedham-Elvidge, G.L. Forster, N.R.P. Harris, M.I. Mead, A.A. Samah, S.M. Phang, C.F. Ou-Yang, N.H. Lin, J.L. Wang, A.K. Baker, C.A.M. Brenninkmeijer, and D. Sherry, A growing threat to the ozone layer from short-lived anthropogenic chlorocarbons, Atmos. Chem. Phys., 17 (19), 11929-11941, doi:10.5194/acp-17-11929-2017, 2017.

Peters, T., ***A Cool World: Defining the Energy Conundrum of Cooling for All***, University of Birmingham, Birmingham Energy Institute, and the Institute for Global

Innovation, Birmingham, United Kingdom, 19 pp., [available at: https://www.birmingham.ac.uk/Documents/college-eps/energy/Publications/2018-clean-cold-report.pdf], 2018.

Pickard, H.M., A.S. Criscitiello, D. Persaud, C. Spencer, D.C.G. Muir, I. Lehnherr, M.J. Sharp, A.O. De Silva, and C.J. Young, Ice core record of persistent short-chain fluorinated alkyl acids: Evidence of the impact from global environmental regulations, ***Geophys. Res. Lett.***, ***47*** (10), e2020GL087535, doi:10.1029/2020gl087535, 2020.

Prinn, R.G., R.F. Weiss, J. Arduini, T. Arnold, H.L. DeWitt, P.J. Fraser, A.L. Ganesan, J. Gasore, C.M. Harth, O. Hermansen, J. Kim, P.B. Krummel, S. Li, Z.M. Loh, C.R. Lunder, M. Maione, A.J. Manning, B.R. Miller, B. Mitrevski, J. Mühle, S. O'Doherty, S. Park, S. Reimann, M. Rigby, T. Saito, P.K. Salameh, R. Schmidt, P.G. Simmonds, L.P. Steele, M.K. Vollmer, R.H. Wang, B. Yao, Y. Yokouchi, D. Young, and L. Zhou, History of chemically and radiatively important atmospheric gases from the Advanced Global Atmospheric Gases Experiment (AGAGE), ***Earth Syst. Sci. Data***, ***10*** (2), 985–1018, doi:10.5194/essd-10-985-2018, 2018.

Pu, J., H. Xu, B. Yao, Y. Yu, Y. Jiang, Q. Ma, and L. Chen, Estimate of hydrofluorocarbon emissions for 2012–16 in the Yangtze River Delta, China, ***Adv. Atm. Sci.***, ***37*** (6), 576–585, doi:10.1007/s00376-020-9242-3, 2020.

Purohit, P., L. Höglund-Isaksson, J. Dulac, N. Shah, M. Wei, P. Rafaj, and W. Schöpp, Electricity savings and greenhouse gas emission reductions from global phase-down of hydrofluorocarbons, ***Atmos. Chem. Phys.***, ***20*** (19), 11,305–11,327, doi:10.5194/acp-20-11305-2020, 2020.

Rayne, S., and K. Forest, Aqueous phase hydration and hydrate acidity of perfluoroalkyl and n:2 fluorotelomer aldehydes, ***J. Environ. Sci. Health A***, ***51*** (7), 579–582, doi:10.1080/10934529.2016.1141625, 2016.

Rigby, M., R.G. Prinn, S. O'Doherty, S.A. Montzka, A. McCulloch, C.M. Harth, J. Mühle, P.K. Salameh, R.F. Weiss, D. Young, P.G. Simmonds, B.D. Hall, G.S. Dutton, D. Nance, D.J. Mondeel, J.W. Elkins, P.B. Krummel, L.P. Steele, and P.J. Fraser, Re-evaluation of the lifetimes of the major CFCs and CH_3CCl_3 using atmospheric trends, ***Atmos. Chem. Phys.***, ***13*** (5), 2691–2702, doi:10.5194/acp-13-2691-2013, 2013.

Rigby, M., R.G. Prinn, S. O'Doherty, B.R. Miller, D. Ivy, J. Mühle, C.M. Harth, P.K. Salameh, T. Arnold, R.F. Weiss, P.B. Krummel, L.P. Steele, P.J. Fraser, D. Young, and P.G. Simmonds, Recent and future trends in synthetic greenhouse gas radiative forcing, ***Geophys. Res. Lett.***, ***41*** (7), 2623–2630, doi:10.1002/2013GL059099, 2014.

Say, D., A.L. Ganesan, M.F. Lunt, M. Rigby, S. O'Doherty, C. Harth, A.J. Manning, P.B. Krummel, and S. Bauguitte, Emissions of halocarbons from India inferred through atmospheric measurements, ***Atmos. Chem. Phys.***, ***19*** (15), 9865–9885, doi:10.5194/acp-2018-1146, 2019.

Schoenenberger, F., S. Henne, M. Hill, M.K. Vollmer, G. Kouvarakis, N. Mihalopoulos, S. O'Doherty, M. Maione, L. Emmenegger, T. Peter, and S. Reimann, Abundance and sources of atmospheric halocarbons in the Eastern Mediterranean, ***Atmos. Chem. Phys.***, ***18*** (6), 4069–4092, doi:10.5194/acp-18-4069-2018, 2018.

Scollard, D.J., J.J. Treacy, H.W. Sidebottom, C. Balestra-Garcia, G. Laverdet, G. LeBras, H. MacLeod, and S. Teton, Rate constants for the reactions of hydroxyl radicals and chlorine atoms with halogenated aldehydes, ***J. Phys. Chem.***, ***97***, 4683–4688, doi:10.1021/j100120a021, 1993.

Scott, B.F., R.W. Macdonald, K. Kannan, A. Fisk, A. Witter, N. Yamashita, L. Durham, C. Spencer, and D.C.G. Muir, Trifluoroacetate profiles in the Arctic, Atlantic, and Pacific oceans, ***Environ. Sci. Technol.***, ***39*** (17), 6555–6560, doi:10.1021/es047975u, 2005.

Sellevåg, S.R., T. Kelly, H. Sidebottom, and C.J. Nielsen, A study of the IR and UV-Vis absorption cross-sections, photolysis and OH-initiated oxidation of CF_3CHO and CF_3CH_2CHO, ***Phys. Chem. Chem. Phys.*** ***6*** (6), ***1243***–1252, doi:10.1039/B315941H, 2004.

Shah, N., M. Wei, V. Letschert, and A. Phadke, ***Benefits of Energy Efficient and Low-Global Warming Potential Refrigerant Cooling Equipment***, No. LBNL-2001229, Lawrence Berkley National Laboratory, Berkeley, California, doi:10.2172/1559243, 2019.

Simmonds, P.G., M. Rigby, A.J. Manning, M.F. Lunt, S. O'Doherty, A. McCulloch, P.J. Fraser, S. Henne, M.K. Vollmer, J. Mühle, R.F. Weiss, P.K. Salameh, D. Young, S. Reimann, A. Wenger, T. Arnold, C.M. Harth, P.B. Krummel, L.P. Steele, B.L. Dunse, B.R. Miller, C.R. Lunder, O. Hermansen, N. Schmidbauer, T. Saito, Y. Yokouchi, S. Park, S. Li, B. Yao, L.X. Zhou, J. Arduini, M. Maione, R.H.J. Wang, D. Ivy, and R.G. Prinn, Global and regional emissions estimates of 1,1-difluoroethane (HFC-152a, CH3CHF2) from in situ and air archive observations, Atmos. Chem. Phys., 16 (1), 365-382, doi: 10.5194/acp-16-365-2016, 2016.

Simmonds, P.G., M. Rigby, A. McCulloch, M.K. Vollmer, S. Henne, J. Mühle, S. O'Doherty, A.J. Manning, P.B. Krummel, P.J. Fraser, D. Young, R.F. Weiss, P.K. Salameh, C.M. Harth, S. Reimann, C.M. Trudinger, P. Steele, R.H.J. Wang, D.J. Ivy, R.G. Prinn, B. Mitrevski, and D.M. Etheridge, Recent increases in the atmospheric growth rate and emissions of HFC-23 (CHF_3) and the link to HCFC-22 ($CHClF_2$) production, ***Atmos. Chem. Phys.***, ***18*** (6), 4153–4169, doi:10.5194/acp-18-4153-2018, 2018.

Simpson, I.J., O.S. Aburizaiza, A. Siddique, B. Barletta, N.J. Blake, A. Gartner, H. Khwaja, S. Meinardi, J. Zeb, and D.R. Blake, Air quality in Mecca and surrounding holy places in Saudi Arabia during Hajj: initial survey, ***Environ. Sci. Technol.***, ***48*** (15), 8529–8537, doi:10.1021/es5017476, 2014.

Solomon, K.R., G.J.M. Velders, S.R. Wilson, S. Madronich, J. Longstreth, P.J. Aucamp, and J.F. Bornman, Sources, fates, toxicity, and risks of trifluoroacetic acid and its salts: Relevance to substances regulated under the Montreal and Kyoto Protocols, ***J. Toxicol. Environ. Health B***, ***19*** (7), 289–304, doi:10.1080/10937404.2016.1175981, 2016.

Stanley, K.M., D. Say, J. Mühle, C.M. Harth, P.B. Krummel, D. Young, S.J. O'Doherty, P.K. Salameh, P.G. Simmonds, R.F. Weiss, R.G. Prinn, P.J. Fraser, and M. Rigby, Increase in global emissions of HFC-23 despite near-total expected reductions, ***Nature Commun.***, ***11*** (1), 397, doi:10.1038/s41467-019-13899-4, 2020.

Stohl, A., Seibert, P., Arduini, J., Eckhardt, S., Fraser, P., Greally, B. R., Lunder, C., Maione, M., Mühle, J., O'Doherty, S., Prinn, R. G., Reimann, S., Saito, T., Schmidbauer, N., Simmonds, P. G., Vollmer, M. K., Weiss, R. F., Yokouchi, Y. An analytical inversion method for determining regional and global emissions of greenhouse gases : Sensitivity studies and application to halocarbons. ***Atmospheric Chemistry and Physics***, ***9***(5), 1597–1620. https://doi.org/10.5194/acp-9-1597-2009, 2009.

Su, S., X. Fang, L. Li, J. Wu, J. Zhang, W. Xu, and J. Hu, HFC-134a emissions from mobile air conditioning in China from 1995 to 2030, ***Atmos. Environ.***, ***102***, 122–129, doi:10.1016/j.atmosenv.2014.11.057, 2015.

Sulbaek Andersen, M.P., J.A. Schmidt, A. Volkova, and D.J. Wuebbles, A three-dimensional model of the atmospheric chemistry of E and Z-CF_3CH=CHCl (HCFO-1233(zd) (E/Z)), ***Atmos. Environ.***, ***179***, 250–259, doi:10.1016/j.atmosenv.2018.02.018, 2018.

Sulbaek Andersen, M.P., and O.J. Nielsen, Tropospheric photolysis of CF_3CHO, ***Atmos. Environ.***, ***272***, 118935, doi:10.1016/j.atmosenv.2021.118935, 2022.

Sung, D.J., D.J. Moon, J. Kim, S. Moon, and S.-I. Hong, Production of TFE by catalytic pyrolysis of chlorodifluoromethane ($CHClF_2$), ***Stud. Surf. Sci. Catal.***, ***159***, 233–236, doi:10.1016/S0167-2991(06)81576-4, 2006.

Takeda, M., H. Nakajima, I. Murata, T. Nagahama, I. Morino, G.C. Toon, R.F. Weiss, J. Mühle, P.B. Krummel, P.J. Fraser, and H.-J. Wang, First ground-based FTIR observations of HFC-23 at Rikubetsu, Japan, and Syowa Station, Antarctica, ***Atmos. Meas. Tech.***, ***14*** (9), 5955–5976, doi:10.5194/amt-2020-505, 2021.

TEAP (Technology and Economic Assessment Panel), Montreal Protocol on Substances that Deplete the Ozone Layer, ***Decision XXXI/7 - Continued Provision of Information on Energy-efficient and Low-global-warming-potential Technologies***, ISBN: 978-9966-076-88-5, [available at: https://ozone.unep.org/system/files/documents/TEAP-EETF-report-may2021.pdf], 2021.

Timatic, ***Timatic Extraction Equipment and Processes: FC Extractor Models***, Timatic USA, [available at: https://timaticusa.com/fcextractioninfo], 2021a.

UNEP (United Nations Environment Programme), Environmental Effects Assessment Panel, ***Environmental Effects of Ozone Depletion and its Interactions with Climate Change: 2014 Assessment***, United Nations Environment Programme, Nairobi, Kenya, [available at: https://ozone.unep.org/sites/default/files/2019-05/eeap_report_2014.pdf], 2014.

UNEP (United Nations Environment Programme), ***Report of the Twenty-Eighth Meeting of the Parties to the Montreal Protocol on Substances that Deplete the Ozone Layer***, UNEP/OzL.Pro.28/12, United Nations Environment Programme, Kigali, Rwanda, [available at: https://ozone.unep.org/sites/default/files/2019-08/MOP-28-12E.pdf], 2016.

UNEP (United Nations Environment Programme), ***2017 Progress Report of the Technology and Economic Assessment Pane***l, coordinated by Maranion, B., M. Pizano, and A. Woodcock, United Nations Environment Programme, Vol. 1, 105 pp., Nairobi, Kenya, [available at: https://ozone.unep.org/sites/default/files/2019-05/TEAP-Progress-Report-May2017.pdf], 2017.

UNEP (United Nations Environment Programme), Executive Committee of the Multilateral Fund for the Implementation of the Montreal Protocol, ***Cost-effective***

Options for Controlling HFC-23 By-product Emissions (Decision 81/68(e)), United Nations Environment Programme, Montreal, Canada, [available at: http://multilateralfund.org/82/English/1/8268.pdf], 2018a.

UNEP (United Nations Environment Programme), Executive Committee of the Multilateral Fund for the Implementation of the Montreal Protocol, *Corrigendum: Cost-effective Options for Controlling HFC-23 By-product Emissions (Decision 81/68(e))*, United Nations Environment Programme, Montreal, Canada, [available at: http://multilateralfund.org/82/English/1/8268c1.pdf], 2018b.

UNEP (United Nations Environment Programme), *Refrigeration, Air Conditioning and Heat Pumps Technical Options Committee: 2018 Assessment Report*, United Nations Environment Programme, ISBN: 978-9966-076-58-8, 300 pp., Nairobi, Kenya, [available at: https://ozone.unep.org/sites/default/files/2019-04/RTOC-assessment-report-2018_0.pdf], 2018c.

UNEP (United Nations Environment Programme), Report of the Technology and Economic Assessment Panel, *Decision XXIX/10--Task Force on Issues Related to Energy Efficiency While Phasing Down Hydrofluorocarbons*, United Nations Environment Programme, Vol. 5, 90 pp., ISBN: 978-9966-076-42-7, Nairobi, Kenya, [available at: https://ozone.unep.org/sites/default/files/2019-04/TEAP_DecisionXXIX-10_Task_Force_EE_May2018.pdf], 2018d.

UNEP (United Nations Environment Programme), Report of the Technology and Economic Assessment Panel, *Decision XXXI/7—Continued Provision of Information on Energy-Efficient and Low-Global-Warming-Potential Technologies*, United Nations Environment Programme, Vol. 2, 127 pp., ISBN: 978-9966-076-86-1, Nairobi, Kenya, [available at: https://ozone.unep.org/sites/default/files/assessment_panels/TEAP_dec-XXXI-7-TFEE-report-september2020.pdf], 2020a.

UNEP (United Nations Environment Programme), Report of the Technology and Economic Assessment Panel, *Assessment of the Funding Requirement for the Replenishment of the Multilateral Fund for the Period 2021-2023*, United Nations Environment Programme, Vol. 3, 108 pp., ISBN: 978-9966-076-84-7, Nairobi, Kenya, [available at: https://ozone.unep.org/system/files/documents/TEAP_decision_XXXI-1_replenishment-task-force-report_may2020.pdf], 2020b.

UNEP (United Nations Environment Programme), Executive Committee of the Multilateral Fund for the Implementation of the Montreal Protocol, *Report of the sub-group on the production sector*, United Nations Environment Programme, Montreal, Canada, [available at: http://multilateralfund.org/84/English/1/8474ri.pdf], 2020c.

UNEP (United Nations Environment Programme) and IEA (International Energy Agency), *Cooling Emissions and Policy Synthesis Report: Benefits of cooling efficiency and the Kigali Amendment*, United Nations Environment Programme, 50 pp., Nairobi, Kenya and Paris, France, [available at: https://iea.blob.core.windows.net/assets/71c8db7e-1137-41ef-99c3-8f2c8d3a5d86/Cooling_Emissions_and_Policy_Synthesis_Report.pdf], 2020d.

UNEP (United Nations Environment Programme), *Production and consumption of ozone depleting substances under the Montreal Protocol*, United Nations Environment Programme, Nairobi, Kenya, [available at: http://ozone.unep.org], 2021.

UNFCCC (United Nations Framework Convention on Climate Change), *National Inventory Submissions 2020 to the United Nations Framework Convention of Climate Change*, UNFCCC Secretariat, Bonn, Germany, [available at: https://unfccc.int/ghg-inventories-annex-i-parties/2020], 2021.

UNFCCC (United Nations Framework Convention on Climate Change), National Inventory Submissions 2019 (eds.), p. last access: May 2019, https://unfccc.int/process-and-meetings/transparency-and-reporting/reporting-and-review-under-the-convention/greenhouse-gas-inventories-annex-i-parties/national-inventory-submissions-2019, 2019.

UNFCCC (United Nations Framework Convention on Climate Change), National Inventory Submissions 2021, https://unfccc.int/ghg-inventories-annex-i-parties/2021, 2021.

US EPA (Environmental Protection Agency), *Phasedown of Hydrofluorocarbons: Establishing the Allowance Allocation and Trading Program Under the American Innovation and Manufacturing Act*, U.S. Environmental Protection Agency, [https://www.federalregister.gov/documents/2021/10/05/2021-21030/phasedown-of-hydrofluorocarbons-establishing-the-allowance-allocation-and-trading-program-under-the], 2021a.

US EPA (U.S. Environmental Protection Agency), *Inventory of U.S. Greenhouse Gas Emissions and Sinks: 1990-2019*, U.S. Environmental Protection Agency, [available at: https://www.epa.gov/ghgemissions/inventory-us-greenhouse-gas-emissions-and-sinks-1990-2019], 2021b.

Velders, G.J.M., S.O. Andersen, J.S. Daniel, D.W. Fahey, and M. McFarland, The importance of the Montreal Protocol in protecting climate, *Proc. Natl. Acad. Sci.*, 104 (12), 4814-4819, doi:10.1073/pnas.0610328104, 2007.

Velders, G.J.M., A.R. Ravishankara, M.K. Miller, M.J. Molina, J. Alcamo, J.S. Daniel, D.W. Fahey, S.A. Montzka, and S. Reimann, Preserving Montreal Protocol Climate Benefits by Limiting HFCs, *Science*, 335 (6071), 922-923, doi:10.1126/science.1216414, 2012.

Velders, G.J.M., D.W. Fahey, J.S. Daniel, S.O. Andersen, and M. McFarland, Future atmospheric abundances and climate forcings from scenarios of global and regional hydrofluorocarbon (HFC) emissions, *Atmos. Environ., 123*, 200–209, doi:10.1016/j.atmosenv.2015.10.071, 2015.

Velders, G.J.M., J.S. Daniel, S.A. Montzka, I. Vimont, M. Rigby, P.B. Krummel, J. Muhle, S. O'Doherty, R.G. Prinn, R.F. Weiss, and D. Young, Projections of hydrofluorocarbon (HFC) emissions and the resulting global warming based on recent trends in observed abundances and current policies, *Atmos. Chem. Phys.*, *22* (9), 6087–6101, doi:10.5194/acp-22-6087-2022, 2022.

Vollmer, M.K., S. Reimann, M. Hill, and D. Brunner, First observations of the fourth generation synthetic halocarbons HFC-1234yf, HFC-1234ze(E), and HCFC-1233zd(E) in the atmosphere, *Environ. Sci. Technol., 49* (5), 2703–2708, doi:10.1021/es505123x, 2015.

Wallington, T.J., W.F. Schneider, D.R. Worsnop, O.J. Nielsen, J. Sehested, W.J. Debruyn, and J.A. Shorter, The environmental impact of CFC replacements HFCs and HCFCs, *Environ. Sci. Technol.*, *28* (7), 320A–326A, doi:10.1021/es00056a714, 1994.

Wang, Z., Y. Wang, J. Li, S. Henne, B. Zhang, J. Hu, and J. Zhang, Impacts of the degradation of 2, 3, 3, 3-tetrafluoropropene into trifluoroacetic acid from its application in automobile air conditioners in China, the United States, and Europe, *Environ. Sci. Technol., 52* (5), 2819–2826, doi:10.1021/acs.est.7b05960, 2018.

WMO (World Meteorological Organization), *Scientific Assessment of Ozone Depletion: 2018*, Global Ozone Research and Monitoring Project–Report No. 58, 588 pp., Geneva, Switzerland, 2018.

Xu, Y., D. Zaelke, G.J.M. Velders, and V. Ramanathan, The role of HFCs in mitigating 21st century climate change, *Atmos. Chem. Phys.*, *13* (12), 6083–6089, doi:10.5194/acp-13-6083-2013, 2013.

Yao, B., X. Fang, M.K. Vollmer, S. Reimann, L. Chen, S. Fang, and R.G. Prinn, China's hydrofluorocarbon emissions for 2011–2017 inferred from atmospheric measurements, *Environ. Sci. Technol. Lett.*, *6* (8), 479–486, doi:10.1021/acs.estlett.9b00319, 2019.

Yvon-Lewis, S.A., and J.H. Butler, Effect of oceanic uptake on atmospheric lifetimes of selected trace gases, *J. Geophys. Res.*, *107* (D20), 4414, doi:10.1029/2001JD001267, 2002.